

Muscle-resident mesenchymal progenitors sense and repair peripheral nerve injury via the GDNF-BDNF axis

Reviewed Preprint

v2 • August 20, 2024

Revised by authors

Reviewed Preprint

v1 • June 4, 2024

Kyusang Yoo, Young-Woo Jo, Takwon Yoo, Sang-Hyeon Hann, Inkuk Park, Yea-Eun Kim, Ye Lynne Kim, Joonwoo Rhee, In-Wook Song, Ji-Hoon Kim, Daehyun Baek, Young-Yun Kong 

School of Biological Sciences, Seoul National University, Seoul 08826, Republic of Korea • Molecular Recognition Research Center, Korea Institute of Science and Technology, Seoul 02792, Republic of Korea

 https://en.wikipedia.org/wiki/Open_access

 Copyright information

Abstract

Fibro-adipogenic progenitors (FAPs) are muscle-resident mesenchymal progenitors that can contribute to muscle tissue homeostasis and regeneration, as well as postnatal maturation and lifelong maintenance of the neuromuscular system. Recently, traumatic injury to the peripheral nerve was shown to activate FAPs, suggesting that FAPs can respond to nerve injury. However, questions of how FAPs can sense the anatomically distant peripheral nerve injury and whether FAPs can directly contribute to nerve regeneration remained unanswered. Here, utilizing single-cell transcriptomics and mouse models, we discovered that a subset of FAPs expressing GDNF receptors *Ret* and *Gfra1* can respond to peripheral nerve injury by sensing GDNF secreted by Schwann cells. Upon GDNF sensing, this subset becomes activated and expresses *Bdnf*. FAP-specific inactivation of *Bdnf* (*Prrx1*^{Cre}; *Bdnf*^{fl/fl}) resulted in delayed nerve regeneration owing to defective remyelination, indicating that GDNF-sensing FAPs play an important role in the remyelination process during peripheral nerve regeneration. In aged mice, significantly reduced *Bdnf* expression in FAPs was observed upon nerve injury, suggesting the clinical relevance of FAP-derived BDNF in the age-related delays in nerve regeneration. Collectively, our study revealed the previously unidentified role of FAPs in peripheral nerve regeneration, and the molecular mechanism behind FAPs' response to peripheral nerve injury.

eLife assessment

The study has identified a cell type in muscle that is characterized as an adipogenic progenitor cell that is capable of promoting regeneration through the action of BDNF, a prominent growth factor regulated by GDNF in Schwann cells. These results represent an **important** cellular explanation for nerve regeneration. The revised analysis is **solid** but the work remains **incomplete** due to a lack of evidence that BDNF is produced during the process through the action of GDNF.

<https://doi.org/10.7554/eLife.97662.2.sa2>

Introduction

Positioned in the interstitial space between myofibers (Uezumi et al., 2010 [DOI](#)), fibro-adipogenic progenitors (FAPs) interact with cellular components within skeletal muscle to ensure normal development, homeostasis, and regeneration of muscle tissue. During developmental myogenesis, embryonic FAPs expressing *Osr1* contribute to limb muscle patterning by regulating the expression of extracellular matrix (ECM) genes that make up muscle connective tissue (Vallecillo-Garcia et al., 2017 [DOI](#)). In young adults, FAPs are necessary for normal growth and long-term maintenance of skeletal muscle, which otherwise undergo progressive muscle atrophy in the absence of PDGFR α ⁺ FAPs (Roberts et al., 2013 [DOI](#); Wosczyzna et al., 2019 [DOI](#); Uezumi et al., 2021 [DOI](#)). Upon muscle injury, FAPs proliferate in response to IL-4/IL-13 signals from eosinophils, and participate in clearing of necrotic debris via phagocytosis (Heredia et al., 2013 [DOI](#)). Also, the proliferated FAPs regulate expansion and asymmetric commitment of muscle stem cells (MuSCs) via secreted factors such as WISP1, leading to robust *de novo* myofiber formation (Joe et al., 2010 [DOI](#); Lukjanenko et al., 2019 [DOI](#); Wosczyzna et al., 2019 [DOI](#)). Conversely, absence of FAPs or its functional decline with age cause premature differentiation of MuSCs upon injury, resulting in formation of smaller regenerated myofibers (Murphy et al., 2011 [DOI](#); Lukjanenko et al., 2019 [DOI](#); Wosczyzna et al., 2019 [DOI](#)). After sufficient regeneration of myofibers occurs, FAPs undergo apoptosis via TNF signaling from monocyte/macrophages, such that its numbers return to those of unperturbed muscles (Lemos et al., 2015 [DOI](#); Saito et al., 2020 [DOI](#)). Failure to remove excess FAPs after muscle regeneration results in unwanted fibrosis, which compromises muscle function (Uezumi et al., 2011 [DOI](#); Uezumi et al., 2014 [DOI](#)).

In addition to formation and maintenance of muscle tissue, FAPs also contribute to maturation and maintenance of the neural components within skeletal muscle. Previously, we reported that FAPs promote postsynaptic maturation of the neuromuscular junction (NMJ) through the BAP1/SMN axis during postnatal development (Kim et al., 2022 [DOI](#)). Selective inactivation of *Bap1* in FAPs results in dysfunctional NMJs, with sustained expression of the immature form of acetylcholine receptor subunit, *AchR γ* , in skeletal muscle (Kim et al., 2022 [DOI](#)). Progressively, these mice exhibit denervation at the NMJ, retraction of motor axons, reduction of myelination and axon diameter, and eventually motor neuron loss, suggesting that FAPs prevent the dying-back loss of motor neurons (Kim et al., 2022 [DOI](#)). Recently, we also reported defective presynaptic maturation and maintenance in mice with selective *Smn* downregulation in FAPs, again suggesting the role of FAPs in postnatal NMJ development (Hann et al., 2024 [DOI](#)). In adult mice, BMP3B secretion by FAPs stabilize NMJs and Schwann cells by promoting the myelination program in Schwann cells, thereby directly contributing to the maintenance of neural components within skeletal muscle (Uezumi et al., 2021 [DOI](#)). In the absence of FAPs or *Bmp3b*, mice exhibit muscle weakness and myofiber atrophy along with destabilization of Schwann cells and denervation at NMJs, which closely resemble the phenotypes observed in age-related sarcopenia (Uezumi et al., 2021 [DOI](#)). Similarly, conditional deletion of *Bap1* in FAPs in adulthood cause denervation at the NMJs and eventually loss of motor neurons, demonstrating the requirement of FAPs in maintaining the neuromuscular system (Kim et al., 2022 [DOI](#)). Conversely, disturbance in the neural component can influence the behavior of FAPs; for instance, denervation is known to activate FAPs (Contreras et al., 2016 [DOI](#); Gonzalez et al., 2017 [DOI](#); Madaro et al., 2018 [DOI](#)). This suggests that FAPs can somehow sense the anatomically distant peripheral nerve injury. However, the question of how FAPs are able to sense the distant peripheral nerve injury remains unanswered (Theret et al., 2021 [DOI](#)). Furthermore, whether FAPs are actually able to exert beneficial effects on peripheral nerve regeneration remains elusive.

In accordance with its various functions, heterogeneity within FAPs began to be recognized with the advent of single-cell analysis technology (Contreras et al., 2021 [DOI](#)). By profiling the expression levels of 87-selected genes in isolated singlets of FAPs, dynamic transitions between heterogeneous

subpopulations of FAPs, identified by different expression levels of TIE2 and VCAM1, was observed during postnatal and regenerative myogenesis (Malecova et al., 2018). The report showed that while activation of TIE2^{high} FAPs is observed in neonatal mice, activation of VCAM1⁺ FAPs is observed in injured muscles, suggesting distinct functional involvement of FAPs in the two different contexts of myogenesis (Malecova et al., 2018). Additionally, single-cell RNA-sequencing (scRNA-seq) enabled identification of heterogeneity within FAPs based on the genome-wide transcriptome data (Lieberman et al., 2021). In homeostatic adult muscle, two distinct subpopulations within FAPs have been identified, namely *Dpp4*⁺ and *Cxcl14*⁺ FAPs (Scott et al., 2019; Opreescu et al., 2020). Functionally, we reported that DPP4⁺ FAPs contribute to maturation and maintenance of the neuromuscular system via the BAP1/SMN axis (Kim et al., 2022). In juvenile muscle, five different subpopulations within FAPs were characterized, each having different contexts of activation and differentiation potentials (Leinroth et al., 2022). *Osr1*⁺ FAPs are precursor cells that can form all other subpopulations; *Clu*⁺ FAPs are most potent in mineralization; *Adam12*⁺ and *Gap43*⁺ FAPs are immune-responsive; and *Hsd11b1*⁺ FAPs respond to nerve transection (Leinroth et al., 2022). The different activation cues and differentiation potentials in each subpopulation of FAPs suggest distinct roles those subsets can play in different contexts of skeletal muscle biology. Indeed, dynamic transcriptomic changes in FAP subpopulations in response to muscle injury (Scott et al., 2019; De Micheli et al., 2020; Opreescu et al., 2020) or denervation (Nicoletti et al., 2020; Proietti et al., 2021; Lin et al., 2022; Nicoletti et al., 2023) have been identified in studies that implemented scRNA-seq analysis. Still, the question of how FAPs may sense the distant nerve injury and whether FAPs can beneficially contribute to nerve regeneration remain largely unknown.

In response to nerve injury, various neurotrophic factors are expressed and secreted by the surrounding cells to facilitate regeneration. One of those neurotrophic factors is GDNF, previously reported to be expressed robustly by Schwann cells upon nerve injury (Hammarberg et al., 1996; Hoke et al., 2002; Arthur-Farraj et al., 2012; Xu et al., 2013; Proietti et al., 2021). Canonical GDNF signaling pathway involves two well-known receptors of GDNF: RET and GFRα1. Binding of GDNF to GFRα1 induces complex formation with the receptor tyrosine kinase (RTK) RET, which initiate the downstream phosphorylation cascade via autophosphorylation upon dimerization (Jing et al., 1996; Treanor et al., 1996; Trupp et al., 1996). The downstream phosphorylation cascades include the Ras-MAPK pathway, the PI3K-Akt pathway, and the Src family kinase-mediated pathway, which are known to promote neuronal survival and neurite outgrowth (Encinas et al., 2001; Sariola and Saarma, 2003). Indeed, exogenous delivery of GDNF was shown to promote motor neuron survival and enhance axonal growth upon nerve injury, which resulted in improved functional recovery (Cintrón-Colón et al., 2020). Though the role and function of GDNF on the regenerating neuron have been demonstrated, other possible cellular targets of GDNF that may facilitate the nerve regeneration process remain to be studied.

Here, using the scRNA-seq approach, we aimed to identify the response mechanism of FAPs to nerve injury, by uncovering its nerve injury-sensing mechanism and its potentially beneficial effect on nerve regeneration. To obtain a comprehensive scRNA-seq database of FAPs' response to nerve injury, FAPs from both chronic, non-regenerating nerve injury (denervation)-and acute, regeneration-prone nerve injury (crush)-affected muscles were collected at different time points over the course of regeneration. As a result, distinct transcriptomic profiles of FAPs at different time points post the two types of nerve injuries were captured in single-cell resolution, from which the response mechanism of FAPs to nerve injury was identified and validated using mouse models. Specifically, we found that upon peripheral nerve injury, GDNF from Schwann cells can activate FAPs, which in turn express BDNF to promote remyelination during nerve regeneration. Our study suggests FAPs as an important player that actively participates in the nerve regeneration process, of which we believe should be considered in future studies aiming for improved understanding of the peripheral nerve regeneration process.

Results

Distinct response profiles of FAPs upon nerve crush injury versus denervation

To establish a comprehensive transcriptome database of nerve injury-affected FAPs at single-cell resolution, we performed scRNA-seq using FAPs isolated from sciatic nerve crush injury (SNC)- or denervation (DEN)-affected muscles at different time points over the course of regeneration (**Figure 1—figure supplements 1A** [↗](#) and **B** [↗](#)). Four time points (3, 7, 14, and 28 days post injury, hereafter dpi) along the regeneration process were chosen for analysis to capture the transcriptomes of FAPs at both early and late stages of regeneration. Selection of such time points was based on a previous report that showed the reinnervation process of the tibialis anterior (TA) muscle after SNC, where Wallerian degeneration was evident at 7 dpi, and reinnervation was mostly completed at 28 dpi (Magill et al., 2007 [↗](#)). Including the uninjured control, scRNA-seq data from a total of nine samples (Uninjured, SNC-3dpi, SNC-7dpi, SNC-14dpi, SNC-28dpi, DEN-3dpi, DEN-7dpi, DEN-14dpi, and DEN-28dpi) were obtained via the 10x Genomics platform (**Figure 1—figure supplement 1A** [↗](#)). Quality control and filtering of the sequenced cells yielded a total of 44,597 cells for further analysis, where 4955.2 ± 1022.8 cells were captured from each sample. Prior to downstream analysis, integration (Hao et al., 2021 [↗](#)) of our scRNA-seq data with a publicly available scRNA-seq data of mononuclear cells from denervated muscles at 0, 2, 5, and 15 dpi (Nicoletti et al., 2023 [↗](#)) was carried out for data validation. Expectedly, most (97.7%) of the filtered cells in our scRNA-seq data clustered with the denervation-affected FAPs in the published scRNA-seq data, confirming the validity of the data produced in our study (**Figure 1—figure supplements 1C** [↗](#) and **D** [↗](#)).

To look into the chronological transcriptomic changes that occur in FAPs in response to SNC or DEN on a global level, we analyzed our scRNA-seq data by samples. Visualization of the scRNA-seq data on uniform manifold approximation and projection (UMAP) plots showed similar changes in the early stages of regeneration (3 and 7 dpi) compared to uninjured FAPs, regardless of the type of injury (**Figure 1A** [↗](#)). However, as FAPs reached later stages of regeneration (14 and 28 dpi), SNC-affected FAPs returned to states similar to uninjured control, while DEN-affected FAPs stayed in the activated state (**Figure 1A** [↗](#)). The similarities and differences observed on the UMAP plots could also be found in the differentially expressed gene (DEG) analyses as well as in the hierarchical clustering analysis using those DEGs (**Figures 1B–E** [↗](#), **Figure 1—figure supplements 2A–C** [↗](#)). As a result of pairwise DEG analyses comparing all nine samples, different numbers of DEGs were identified, of which correlated with the similarities between samples observed on UMAP plots (**Figures 1A–E** [↗](#), **Figure 1—figure supplements 2A** [↗](#) and **B** [↗](#)). Hierarchical clustering of the nine samples using all unique DEGs identified from the pairwise comparisons showed clustering of uninjured control with SNC-14dpi and SNC-28dpi, suggesting FAPs' return to homeostatic state (**Figure 1—figure supplement 2C** [↗](#)). On the other hand, DEN-14dpi and DEN-28dpi clustered with each other, but not with uninjured control, suggesting the chronic activation of FAPs in response to DEN as reported previously (Madaro et al., 2018 [↗](#)) (**Figure 1—figure supplement 2C** [↗](#)). Samples that captured the early responses of FAPs to nerve injuries (3 or 7 dpi) were clustered together by dpi rather than the type of injury, suggesting similar response profiles of FAPs to both types of nerve injuries (**Figure 1—figure supplement 2C** [↗](#)). Indeed, the numbers of DEGs between SNC-3dpi versus DEN-3dpi and SNC-7dpi versus DEN-7dpi were among the lowest identified in the pairwise analyses (**Figures 1B** [↗](#) and **C** [↗](#), **Figure 1—figure supplement 2A** [↗](#)). Overall, the number of DEGs between SNC- and DEN-affected FAPs increased significantly with dpi, showing the bifurcation of FAP's response to the different types of nerve injuries in the later stages of regeneration (**Figures 1B–E** [↗](#)).

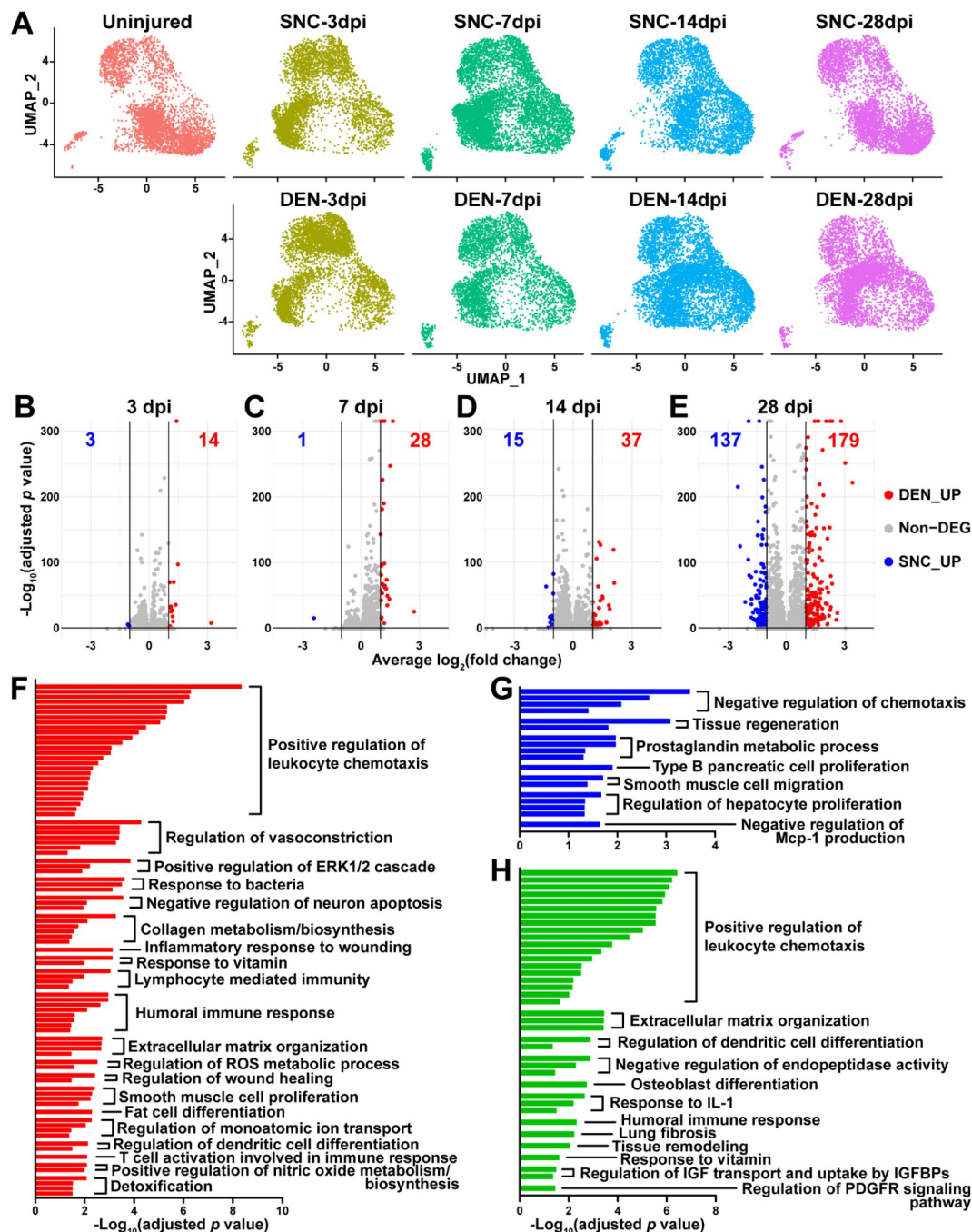


Figure 1.

Distinct response profiles of FAPs upon nerve crush injury versus denervation.

(A) Single-cell transcriptome data of nerve injury-affected FAPs displayed separately by samples on UMAP plots. See **Figure 1—figure supplement 1A** for experimental design. (B–E) Volcano plots showing different numbers of DEGs identified from comparing SNC-vs DEN-affected FAPs at (B) 3, (C) 7, (D) 14, (E) 28 days post injury (dpi). (F–H) Pathway terms enriched from gene set overrepresentation analyses using g:Profiler. DEGs used as input were (F) DEN-28dpi-upregulated versus SNC-28dpi, (G) SNC-28dpi-upregulated versus DEN-28dpi, and (H) DEGs upregulated commonly in SNC-3dpi, SNC-7dpi, DEN-3dpi, and DEN-7dpi versus uninjured control.

In a previous study, chronic activation of the STAT3/IL-6 pathway in FAPs in response to DEN was reported (Madaro et al., 2018 [DOI](#)). Indeed, *Il6* was identified as one of the genes upregulated at all four time points in response to DEN compared to uninjured control in our data (**Figure 1—figure supplements 2D** [DOI](#) and **E** [DOI](#)). Although it did not pass the fold change (FC) threshold ($FC \geq 2$) in the DEG analyses, expression of *Stat3* also showed significant chronic upregulation in all DEN-affected FAPs as well (**Figure 1—figure supplements 2F** [DOI](#) and **G** [DOI](#)). In response to SNC, however, only transient upregulation of both genes was observed (**Figure 1—figure supplements 2D–G** [DOI](#)).

To obtain biological insights on the different responses of FAPs to SNC versus DEN in the later stage of regeneration, we subjected the two lists of genes from **Figure 1E** [DOI](#) (28 dpi, SNC_UP and DEN_UP) to gene set overrepresentation analysis (ORA) using g:Profiler (Kolberg et al., 2023 [DOI](#)). From both sets of genes, pathways related to tissue regeneration/wound healing were enriched (**Figures 1F** [DOI](#) and **G** [DOI](#), **Figure 1—figure supplements 3A** [DOI](#) and **B** [DOI](#)). In contrast, pathways related to immune cell recruitment, inflammation, and ECM regulation by collagen biosynthesis were enriched specifically in DEN-28dpi (**Figure 1F** [DOI](#), **Figure 1—figure supplement 3A** [DOI](#)), which is consistent with the previous report that showed the direct contribution of FAPs to fibrosis in denervated muscles (Contreras et al., 2016 [DOI](#); Madaro et al., 2018 [DOI](#)). Also, mild immune cell infiltration into affected muscles in response to DEN was previously described (Lin et al., 2022 [DOI](#); Nicoletti et al., 2023 [DOI](#)); our results suggest the role of FAPs in chemotactic recruitment of immune cells in denervated muscles. In addition, the pathway ‘negative regulation of neuron apoptosis’ was enriched in DEN-28dpi, suggesting a prolonged attempt of FAPs to preserve neurons that must be alive for reinnervation of the denervated muscle (**Figure 1F** [DOI](#), **Figure 1—figure supplement 3A** [DOI](#)). On the other hand, some pathways were exclusively enriched in SNC-28dpi, such as negative regulation of chemotaxis and prostaglandin metabolism (**Figure 1G** [DOI](#), **Figure 1—figure supplement 3B** [DOI](#)). It is generally understood that after a successful tissue regeneration process, resolution of immune response allow for the tissue to return to homeostasis (Ortega-Gomez et al., 2013 [DOI](#); Aurora and Olson, 2014 [DOI](#); Julier et al., 2017 [DOI](#)); our results suggest the role of FAPs in regulating immune resolution near the end of nerve regeneration. Furthermore, the role of prostaglandin in peripheral nerve regeneration has recently been described (Forese et al., 2020 [DOI](#); Bakooshli et al., 2023 [DOI](#)); our ORA results suggested that FAPs may also be involved in regulation of prostaglandin levels during peripheral nerve regeneration.

To discover biological pathways behind the supposedly similar responses of FAPs to both SNC and DEN in the early phases of regeneration, we examined DEGs from comparing SNC-3dpi, SNC-7dpi, DEN-3dpi, and DEN-7dpi to uninjured controls. Many of the upregulated genes identified in the DEG analyses were shared amongst the four samples (**Figure 1—figure supplement 3C** [DOI](#)). ORA using the shared upregulated genes revealed enrichment in pathways that were also enriched in DEN-28dpi compared to SNC-28dpi, such as immune cell recruitment and ECM regulation, supporting the idea that early-activated states within FAPs persist for a prolonged period in response to DEN (**Figures 1F** [DOI](#) and **H** [DOI](#), **Figure 1—figure supplements 3A** [DOI](#) and **D** [DOI](#)). Collectively, analysis of our scRNA-seq data by samples revealed similar response profiles of FAPs to both SNC and DEN in the early stages of regeneration, which then bifurcated into chronic activation in response to DEN and return to homeostasis in response to SNC, showing correlative behaviors along with the degree of nerve regeneration and target muscle reinnervation.

Nerve injury-responsive subsets within FAPs

Although analysis of our scRNA-seq data on the population level provided general insights on how FAPs may respond to the different types of nerve injuries, the results could not provide us with sufficient clues on how FAPs can sense nerve injuries, or how they may directly contribute to nerve regeneration. Thus, we next analyzed our scRNA-seq data on the subpopulation level, hoping to distinguish subsets within FAPs that may be more relevant to the context of sensing and responding to nerve injury. To identify distinct subsets within nerve injury-affected FAPs, we applied unsupervised clustering to the merged scRNA-seq data of all nine samples following the

Seurat-R workflow (Hao et al., 2021 [↗](#)). As a result, seven clusters with unique gene expression profiles were identified from the nerve injury-affected FAPs, with marker genes specifically expressed in each cluster (**Figures 2A–C** [↗](#), **Figure 2—figure supplement 1A** [↗](#)).

Interestingly, while clusters 4–7 showed little or no significant change in their proportions in response to nerve injury, clusters 1–3 exhibited dramatic changes upon nerve injury (**Figures 2D** [↗](#) and **E** [↗](#)). In particular, cluster 1 was mostly present in uninjured muscles or in muscles where reinnervation had occurred to at least some degree (SNC-14dpi and SNC-28dpi) (Magill et al., 2007 [↗](#)) (**Figures 2D** [↗](#) and **E** [↗](#)). In contrast, presence of clusters 2 and 3 were mutually exclusive to cluster 1, such that their appearances were transient in response to SNC and chronic upon DEN (**Figures 2D** [↗](#) and **E** [↗](#)). Based on this mutual exclusivity of the three clusters, we speculated that cluster 1 can sense and respond to nerve injuries, and that clusters 2 and 3 may have arisen from cluster 1 upon nerve injury.

To obtain clues on whether such changes between FAP clusters could have actually occurred in response to nerve injury, we first performed RNA velocity analysis using R package *velocyto.R* (La Manno et al., 2018 [↗](#)). RNA velocities on the UMAP plots predicted transcriptomic flow from cluster 1 to clusters 2 and 3 in the early stages of regeneration in both SNC- and DEN-affected FAPs, which was in line with our speculation (**Figure 2—figure supplement 1B** [↗](#)). Conversely, transcriptomic flow from clusters 2 and 3 back to cluster 1 was evident in SNC-affected FAPs in the later stages of regeneration (**Figure 2—figure supplement 1B** [↗](#)). However, RNA velocities in DEN-affected FAPs were represented as dots instead of arrows on clusters 2 and 3 in the later stages, suggesting an unchanging, chronic state of their transcriptomes, which is consistent with the chronic activation of FAPs in response to DEN (Madaro et al., 2018 [↗](#)) (**Figure 2—figure supplement 1B** [↗](#)). Additionally, hierarchical clustering of the seven FAP clusters using DEGs enriched in each cluster grouped clusters 1–3 together, supporting our speculation that clusters 2 and 3 originate from cluster 1 (**Figure 2—figure supplement 1C** [↗](#)). Recently, *Hsd11b1*-expressing FAPs were identified as the FAP subset that is specifically activated in response to nerve transection injury (Leinroth et al., 2022 [↗](#)). Since we speculated that cluster 1 in our scRNA-seq data can sense and respond to nerve injury, we examined the expressions of marker genes identified in the previous report – *Hsd11b1*, *Mme*, *Ret*, and *Gfra1* (Leinroth et al., 2022 [↗](#)) – in our scRNA-seq data. Indeed, all four markers were enriched in cluster 1 in our data (**Figures 3A** [↗](#) and **B** [↗](#), **Figure 2—figure supplements 1D–F** [↗](#)). Expressions of marker genes *Hsd11b1* and *Mme* were also enriched in clusters 2 and 3, further supporting the idea that those clusters may have arisen from cluster 1 (**Figure 2—figure supplements 1D–F** [↗](#)). Together, these data suggest that clusters 1–3 are the dynamic interchanging subsets of FAPs that specifically respond to nerve injury, where cluster 1 senses nerve injuries in unperturbed muscles and clusters 2 and 3 arise from cluster 1 to respond to nerve injury.

GDNF signaling pathway in the nerve injury-sensing mechanism by FAPs

Among the four marker genes expressed in cluster 1, *Ret* and *Gfra1* are well-known as GDNF receptors, where GFRα1 directly binds GDNF, which in turn activates the RTK RET for downstream signal transduction (Jing et al., 1996 [↗](#); Treanor et al., 1996 [↗](#); Trupp et al., 1996 [↗](#)). Meanwhile, robust but specific expression of GDNF by Schwann cells in response to peripheral nerve injury has been reported (Hammarberg et al., 1996 [↗](#); Hoke et al., 2002 [↗](#); Arthur-Farraj et al., 2012 [↗](#); Xu et al., 2013 [↗](#); Proietti et al., 2021 [↗](#)). Accordingly, we presumed that FAPs, especially the *Ret*- and *Gfra1*-expressing cluster 1 cells, may sense the distant nerve injury by detecting GDNF secreted from Schwann cells. Notably, both *Ret* and *Gfra1* were among the top 10 DEGs specifically enriched in cluster 1, suggesting that they can readily respond to GDNF (**Figure 2C** [↗](#), **Figure 3—figure supplement 1A** [↗](#)). In addition, comparing the expression levels of *Ret* and *Gfra1* in skeletal muscle-resident mononuclear cell populations isolated by fluorescence-activated cell sorting

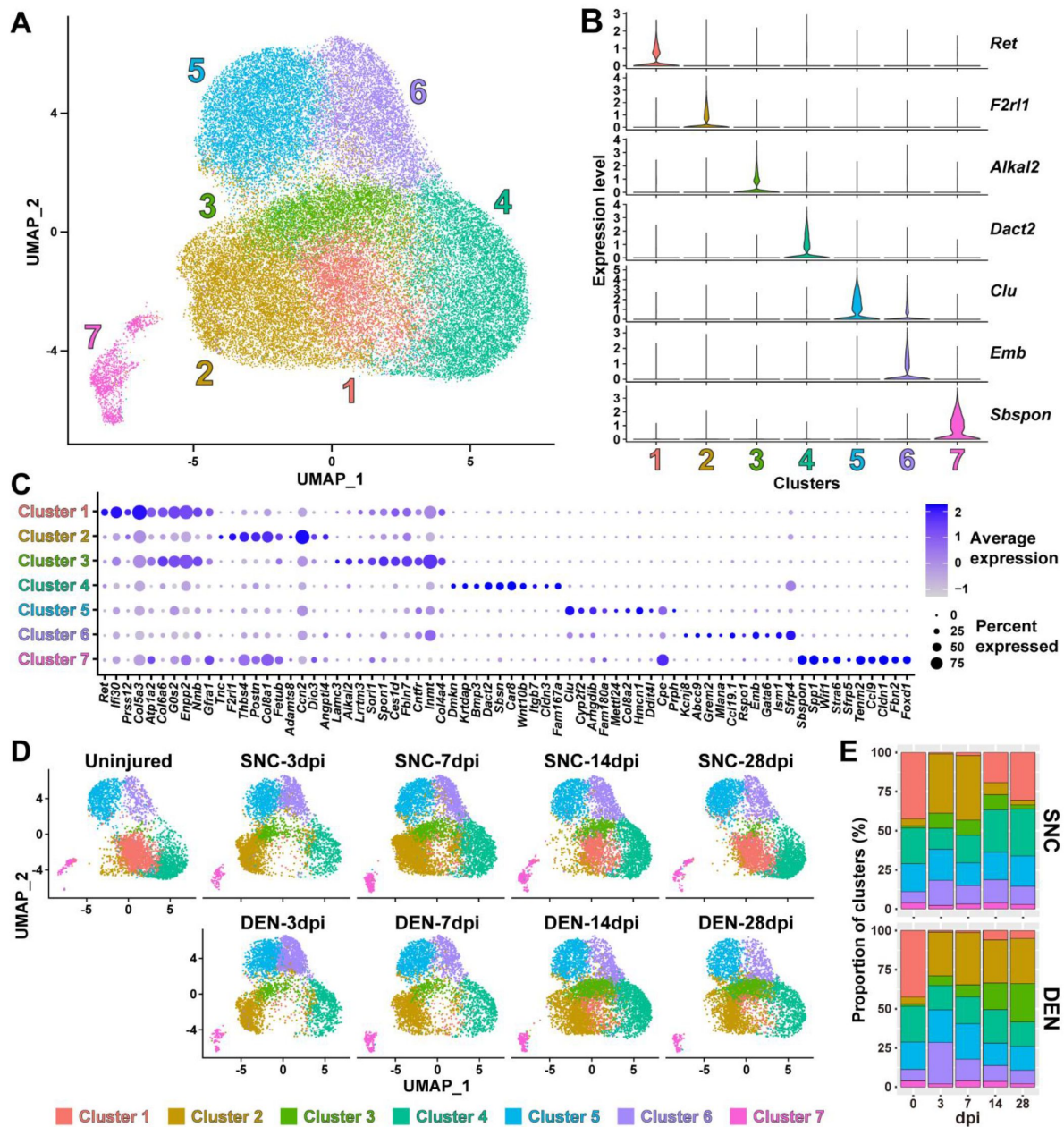


Figure 2.

Nerve injury-responsive subsets within FAPs.

(A) Seven clusters identified by unsupervised clustering using all nine scRNA-seq samples obtained in this study displayed on the UMAP plot. (B) Violin plots showing expressions of unique marker genes identified in each cluster. (C) Dotplot showing the expression levels and percentages of top 10 DEGs enriched in each cluster. (D) UMAP plots of clustered scRNA-seq data displayed separately by samples. (E) Barplots showing the proportions of the seven clusters that comprise each scRNA-seq sample of nerve injury-affected FAPs. For 0 dpi, data from the same uninjured control sample is displayed for both SNC and DEN.

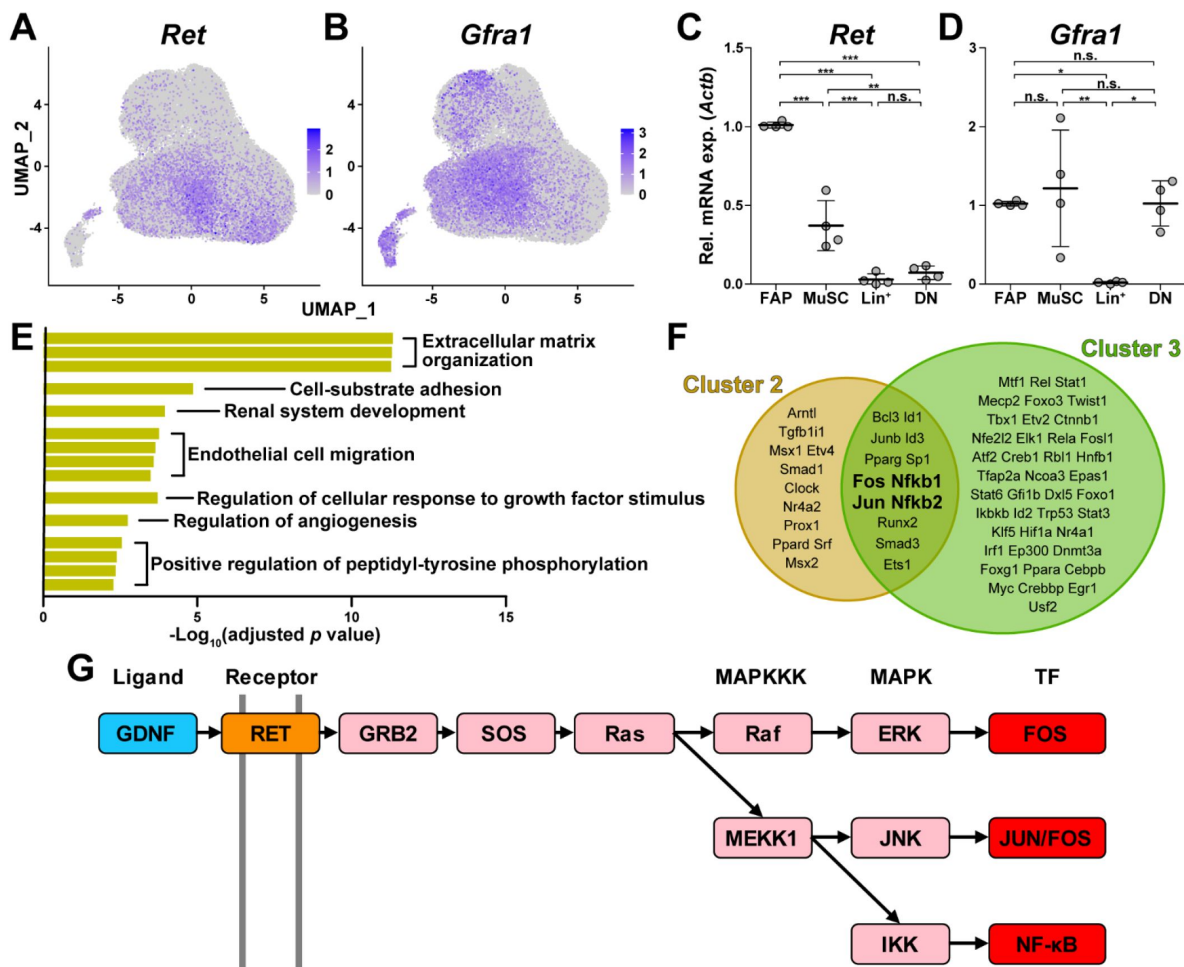


Figure 3.

GDNF signaling pathway in the nerve injury-sensing mechanism by FAPs.

(A–B) UMAP plots showing the expressions of (A) *Ret* and (B) *Gfra1* in the merged scRNA-seq data. (C–D) RT-qPCR results showing the expressions of (C) *Ret* and (D) *Gfra1* in mononuclear cells isolated from uninjured muscles by FACS. See **Figure 1—figure supplement 1B** for the FACS isolation scheme. MuSC, muscle stem cells; Lin⁺, lineage-positive cells; DN, Vcam1/Sca1 double-negative cells. n = 4; one-way ANOVA with Bonferroni's post hoc test. * $p < 0.05$, ** $p < 0.01$, *** $p < 0.001$, n.s., not significant. (E) Shared pathway terms commonly identified from gene set overrepresentation analyses using DEGs specifically upregulated in clusters 1, 2 or 3. See **Figure 3—figure supplements 1B**, **2A**, and **2B** for the full ORA results. (F) Venn diagram showing the results from TRRUST analyses using DEGs enriched in clusters 2 and 3. Transcription factors predicted to regulate genes upregulated in each cluster are listed. (G) Simplified diagram of the GDNF/RET-MAPK signaling pathway. Blue: GDNF ligand; orange: GDNF receptor RET expressed in cluster 1; pink: downstream cascade genes expressed in clusters 1-3; red: transcription factors commonly predicted to regulate upregulated genes in clusters 2 and 3.

(FACS) revealed robust co-expression of both genes in FAPs, but not as much in other cell populations (**Figures 3C** and **D**). Thus, FAPs may be the main cell type within skeletal muscle that can respond to GDNF secreted by Schwann cells in case of a nerve injury.

To further investigate the relevance of GDNF signaling in the nerve injury-sensing mechanism by FAPs, we subjected lists of DEGs enriched in clusters 1-3 to ORA. Genes enriched in cluster 1 returned pathways ‘GDNF receptor signaling pathway’, ‘regulation of cellular response to growth factor stimulus’, and ‘positive regulation of peptidyl-tyrosine phosphorylation’, where tyrosine residues on the RTK RET is known to be phosphorylated upon activation (Jing et al., 1996; Treanor et al., 1996; Trupp et al., 1996) (**Figure 3—figure supplement 1B**). The two latter pathways were also found in the ORA results using DEGs enriched in clusters 2 and 3, supporting the idea that those clusters originate from cluster 1 upon nerve injury (**Figure 3E**, **Figure 3—figure supplements 2A** and **B**). The pathway ‘positive regulation of ERK1/2 cascade’ was enriched in cluster 2, suggesting the involvement of GDNF-RET-Ras-ERK signaling cascade within the MAPK signaling pathway in this cluster, which is one of the known downstream pathways of canonical GDNF signaling (Airaksinen and Saarma, 2002; Sariola and Saarma, 2003; Kanehisa et al., 2023) (**Figure 3G**, **Figure 3—figure supplements 1C** and **2A**). In addition to ORA, we predicted upstream transcription factors (TFs) that could have regulated the expressions of the DEGs enriched in the two activated FAP subsets, clusters 2 and 3, using TRRUST (Han et al., 2018). As a result, TFs *Fos*, *Jun* and *NF-κB* (*Nfkb1*, *Nfkb2*) were predicted from both lists of DEGs, all of which are known to act downstream of the GDNF/RET-induced MAPK signaling pathway (Fielder et al., 2018; Kanehisa et al., 2023) (**Figures 3F** and **G**, **Figure 3—figure supplement 1C**, **Supplemental tables 1** and **2**). Collectively, robust and specific co-expression of GDNF receptors in cluster 1, together with the prediction of RTK activation and involvement of GDNF signaling pathway downstream TFs in clusters 2 and 3, suggests that GDNF signaling could be the mechanism by which FAPs sense the distant nerve injury, where local Schwann cells act as the GDNF source upon nerve injury.

The GDNF-BDNF axis as FAP’s response mechanism to nerve injury

Next, to discover how FAPs may contribute to nerve regeneration, we screened the list of genes enriched in clusters 2 and 3 that were predicted to be downstream of the GDNF signaling pathway to identify candidate effector genes. From the TRRUST analysis results, 44 genes were identified to be regulated by either *Fos*, *Jun*, or *NF-κB* (**Figure 4A**, **Supplemental tables 1–3**). Since FAPs themselves do not constitute the neural components within skeletal muscle, we reasoned that secreted factors from FAPs would most likely exert beneficial effect on the regenerating nerves. Also, considering the effector gene’s potential function in supporting nerve regeneration, we presumed that it regulates neurons or glial cells. Moreover, we anticipated that expression of the effector gene would be limited to the context of nerve injury and regeneration, since the vast majority of FAPs are in a quiescent state in unperturbed adult muscles (Scott et al., 2019). Thus, we applied the following criteria to narrow down our candidate gene list: (1) genes that are known to code secreted proteins, (2) genes that are known to regulate neurons or glial cells, and (3) genes that are expressed exclusively in activated FAPs in response to nerve injury (**Figure 4A**, **Supplemental table 3**). Unexpectedly, after filtering out genes that did not fit the three criteria, only *Bdnf* remained in our candidate gene list that could act as the effector secreted by FAPs upon nerve injury to support nerve regeneration (**Figure 4A**). Expression patterns of *Bdnf* in FAPs upon nerve injury showed transient upregulation in SNC-affected FAPs, whereas chronic expression of *Bdnf* was observed in DEN-affected FAPs, showing correlation with its potential requirement during nerve regeneration (**Figure 4C**). The expression of *Bdnf* was mostly limited to cluster 2 (**Figure 4B**), where pathway analysis and TF prediction suggested the involvement of GDNF-RET-Ras-ERK-Fos signaling cascade in this subset of FAPs (**Figures 3F** and **G**, **Figure 3—figure supplements 1C** and **2A**). Accordingly, we hypothesized that FAPs secrete BDNF in response to GDNF from Schwann cells upon nerve injury, to actively take part in the regeneration process.

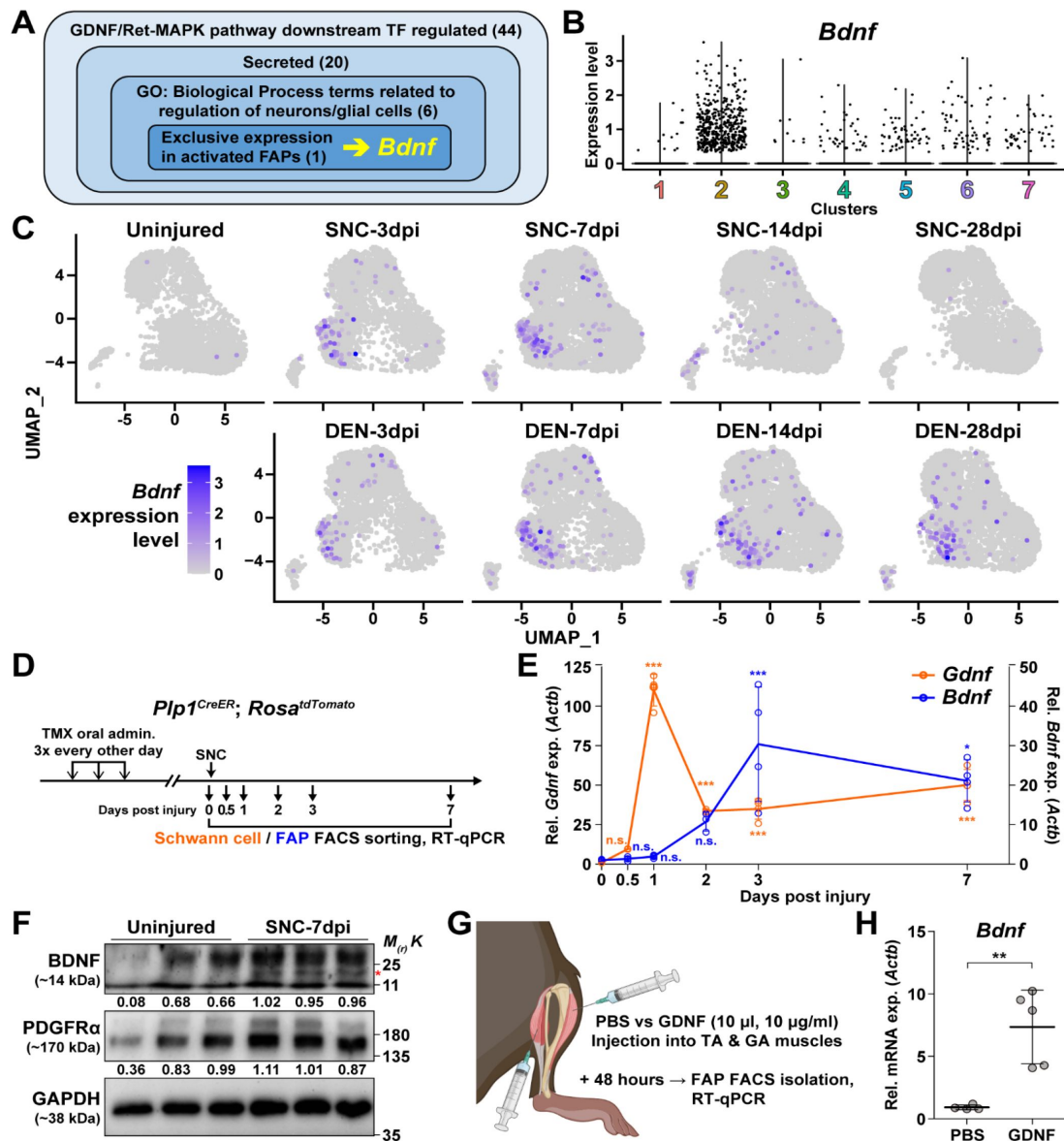


Figure 4.

The GDNF-BDNF axis as FAP's response mechanism to nerve injury.

(A) Identification of candidate genes expressed in FAPs in response to GDNF that may contribute to nerve regeneration. Number of genes that fit into each criterion is indicated. (B) Violin plot displaying the expression levels of *Bdnf* in the seven FAP clusters. (C) Expression of *Bdnf* in each scRNA-seq sample shown on UMAP plots. (D) Scheme for sampling Schwann cells and FAPs at different time points post SNC for gene expression analyses. (E) RT-qPCR results showing expression levels of *Gdnf* in Schwann cells (orange dot and line, left y-axis) and *Bdnf* in FAPs (blue dot and line, right y-axis) at different time points post SNC. $n = 4$, except for 0 and 2 dpi, where $n = 3$. One-way ANOVA with Bonferroni's post hoc test. $* p < 0.05$, $*** p < 0.001$, n.s., not significant. (F) Western blot results showing BDNF protein expression in PDGFR α ⁺ FAPs isolated from SNC-affected or uninjured contralateral muscles at 7 dpi. $n = 3$. Mature form of BDNF is indicated with a red asterisk. Quantified values normalized to GAPDH is indicated below each protein. See **Figure 4—figure supplement 1** for the experimental scheme. (G) Scheme for intramuscular injection of either PBS or recombinant mouse GDNF protein, with the time point for FAP isolation post injection indicated. (H) RT-qPCR results showing the expression level of *Bdnf* in FAPs 48 hours post intramuscular injection of either PBS ($n = 4$) or GDNF ($n = 5$). Unpaired t-test with Welch's correction. $** p < 0.01$.

© 2024, BioRender Inc. Any parts of this image created with *BioRender* are not made available under the same license as the Reviewed Preprint, and are © 2024, BioRender Inc.

To validate our hypothesis *in vivo*, we first examined the expression profiles of *Gdnf* in Schwann cells and *Bdnf* in FAPs at early time points in response to SNC, using *Plp1^{CreER}; Rosa^{tdTomato}* mice to specifically label and hence isolate Schwann cells (Doerflinger et al., 2003) (Figure 4D). Expectedly, we could observe sequential upregulation of *Gdnf* and *Bdnf* from Schwann cells and FAPs, respectively, where *Gdnf* levels peaked at 1 dpi in Schwann cells, followed by a gradual increase of *Bdnf* expression in FAPs, which peaked at 3 dpi (Figures 4D and E). Following mRNA expression validation *in vivo*, we performed western blot analysis using FAPs isolated from either SNC-affected muscles at 7 dpi or from the contralateral, uninjured muscles to validate the expression of BDNF protein upon nerve injury (Figure 4—figure supplement 1). FAPs from both uninjured muscles and SNC-affected muscles showed robust expression of PDGFR α , a well-known marker for FAPs (Joe et al., 2010; Uezumi et al., 2010), indicating successful isolation and protein extraction from the sorted FAPs (Figure 4F). However, unlike PDGFR α , the mature form of BDNF protein could only be detected in SNC-affected FAPs, but not in uninjured FAPs, showing correlative results with the mRNA expression pattern of *Bdnf* in FAPs upon nerve injury (Figures 4E and F). These results demonstrate the expression of BDNF in nerve injury-affected FAPs, but not in uninjured FAPs, on both mRNA and protein levels.

Next, to validate the sufficiency of GDNF signaling in inducing *Bdnf* expression in FAPs *in vivo*, we injected recombinant mouse GDNF protein into the TA and the two gastrocnemius (GA) muscles (lateral and medial GA), from which FAPs were FACS-isolated 48 hours post injection to investigate the expression of *Bdnf* (Figure 4G). Compared to PBS control, intramuscular injection of GDNF sufficiently induced *Bdnf* expression in FAPs, even in the absence of a nerve injury (Figures 4G and H). Conversely, to show the necessity of GDNF signaling in the upregulation of *Bdnf* in FAPs upon nerve injury, we injected either IgG control or anti-GDNF antibodies into the TA and GA muscles 24 hours after SNC, and FACS-isolated FAPs 48 hours post injection for analysis. Though the results were not statistically significant, injection of GDNF blocking antibodies showed a tendency to reduce *Bdnf* expression compared to IgG-injected controls, which is in support of our hypothesis (Figure 4—figure supplement 2). Together, we suggest that FAPs can respond to nerve injury via the GDNF-BDNF axis, since recombinant GDNF protein could sufficiently induce *Bdnf* expression in FAPs without nerve injury, and reduced GDNF activity could weaken *Bdnf* expression in the nerve injury-affected FAPs.

Remyelination by FAP-derived BDNF during peripheral nerve regeneration

Although BDNF is known to function in processes such as axon elongation (Oudega and Hagg, 1999; English et al., 2013), survival of neurons (Ghosh et al., 1994; Baydyuk and Xu, 2014), and myelination by Schwann cells (Zhang et al., 2000; Chan et al., 2001; Xiao et al., 2009), the role of BDNF secreted by FAPs in nerve regeneration is unknown. To find out how FAP-derived BDNF can contribute to nerve regeneration, we produced conditional knockout (cKO) mice where *Bdnf* is specifically inactivated in mesenchymal progenitors including FAPs, by crossing *Prrx1^{Cre}* mice (Logan et al., 2002; Kim et al., 2022; Leinroth et al., 2022; Hann et al., 2024) with *Bdnf*-floxed (*Bdnf^{fl}*) mice (*Prrx1^{Cre}; Bdnf^{fl}*, hereafter cKO) (Figure 5—figure supplement 1A). Inactivation of *Bdnf* in FAPs in the cKO mice was confirmed on both genomic DNA and mRNA levels (Figure 5—figure supplements 1B and C). Though Cre expression in *Prrx1*-expressing cells occur from embryonic day 9.5 (Logan et al., 2002), no visible phenotypes were observed in the postnatal, juvenile and adult cKO mice compared to littermate controls (hereafter, Ctrl). However, upon SNC in the right hindlimb, cKO mice displayed a delay in nerve regeneration compared to Ctrl, measured by compound muscle action potential (CMAP) amplitude and latency via electromyography (EMG) on the GA muscle (Figures 5A–5D, Figure 5—figure supplements 1D and E). At 4 weeks post injury (wpi), nerve regeneration in both Ctrl and cKO mice showed insufficient recovery in the right, injured GA compared to the left, uninjured GA, where lower amplitude and prolonged latency in CMAP was observed (Figures 5B–D). However, at 6 wpi, while CMAP amplitude and latency in the left and right GAs became comparable in Ctrl mice,

recovery of such values were stalled at levels comparable to 4 wpi in the cKO mice (**Figures 5B–D**). By 12 wpi, electrophysiological functions of the injured nerves became statistically comparable to that of its contralateral counterpart in the cKO mice, indicating a delayed regeneration in the cKO mice (**Figures 5B–D**).

Generally, decrease in CMAP amplitude and prolonged CMAP latency can be explained by two main causes: axonal loss and defective myelination (Mallik and Weir, 2005; Chung et al., 2014). Since complete regeneration of the injured nerves on the electrophysiological level could be achieved after a sufficient period of time in the cKO mice (**Figures 5B–D**), we presumed that axonal loss would not have occurred, since it would result in permanent defects by loss of motor units. Instead, we thought that defective myelination could have occurred in the cKO mice, considering the fact that BDNF is already known to promote remyelination during peripheral nerve regeneration (Zhang et al., 2000; Chan et al., 2001; Zheng et al., 2016), and that defective myelination alone can affect both CMAP amplitude and latency (Mallik and Weir, 2005). Thus, we investigated the effect of conditional *Bdnf* inactivation in FAPs on regenerative myelination by examining the sciatic nerves from Ctrl versus cKO mice at 6 wpi, when the delayed functional recovery of the injured nerves in the cKO mice was prominent (**Figures 5A–D**). Toluidine blue staining of the semi-thin sections of injured sciatic nerves revealed significantly reduced myelin thickness in the cKO mice compared to Ctrl mice (**Figure 5E**). Indeed, higher G-ratio values were calculated from cKO mice compared to Ctrl, confirming the reduced myelination in the regenerating nerves in cKO mice (**Figure 5F**, **Figure 5—figure supplements 1F–H**). This decrease in myelin thickness was independent from axon diameter, which were comparable in both Ctrl and cKO mice, implying that no axonal loss or defect had occurred in the cKO mice compared to controls (**Figure 5G**). Taken together, our results revealed the direct involvement of FAP-derived BDNF in the remyelination process during peripheral nerve regeneration, such that inadequate levels of *Bdnf* expression in FAPs caused delayed remyelination and hence delayed nerve regeneration in the cKO mice.

Implication of FAP-derived BDNF in the age-related delay in nerve regeneration

Finally, to seek clinical relevance of *Bdnf* expression in FAPs during nerve regeneration, we compared the expression levels of *Bdnf* in adult (5–6 months) versus aged (24 months) mice in FAPs post SNC. At 7 dpi, *Bdnf* expression was significantly reduced in the aged mice compared to adult mice (**Figures 6A** and **B**). Such a difference could be one of the factors that lead to the delayed or failed regeneration of injured nerves in the elderly compared to healthy, young adults, suggesting the clinical role of FAPs in a timely, successful peripheral nerve regeneration process.

Discussion

Traumatic injury to the peripheral nerve has severe consequences, including lifelong paralysis of the injured limb that can compromise the quality of life significantly (Grinsell and Keating, 2014). Thus, understanding the regeneration process of the peripheral nerves is fundamental for treating the potentially devastating injury. Previously, several cellular components in and outside the injured nerve were discovered to actively participate in the regeneration process, including the injured neurons (Hanz et al., 2003), glial cells (Arthur-Farraj et al., 2012), immune cells (Mueller et al., 2001; Kalinski et al., 2020), and nerve-resident mesenchymal cells (Parrinello et al., 2010; Toma et al., 2020), via diverse mechanisms so that the nerve can regain its function (Scheib and Hoke, 2013). In this study, we investigated the response mechanism of muscle-resident FAPs to both acute and chronic peripheral nerve injury via scRNA-seq, and revealed that this population of cells can also actively take part in the nerve regeneration process. Here, we discovered that muscle-resident FAPs can recognize the distant nerve injury by sensing GDNF secreted by Schwann cells. Though GDNF secretion by Schwann cells in response to nerve

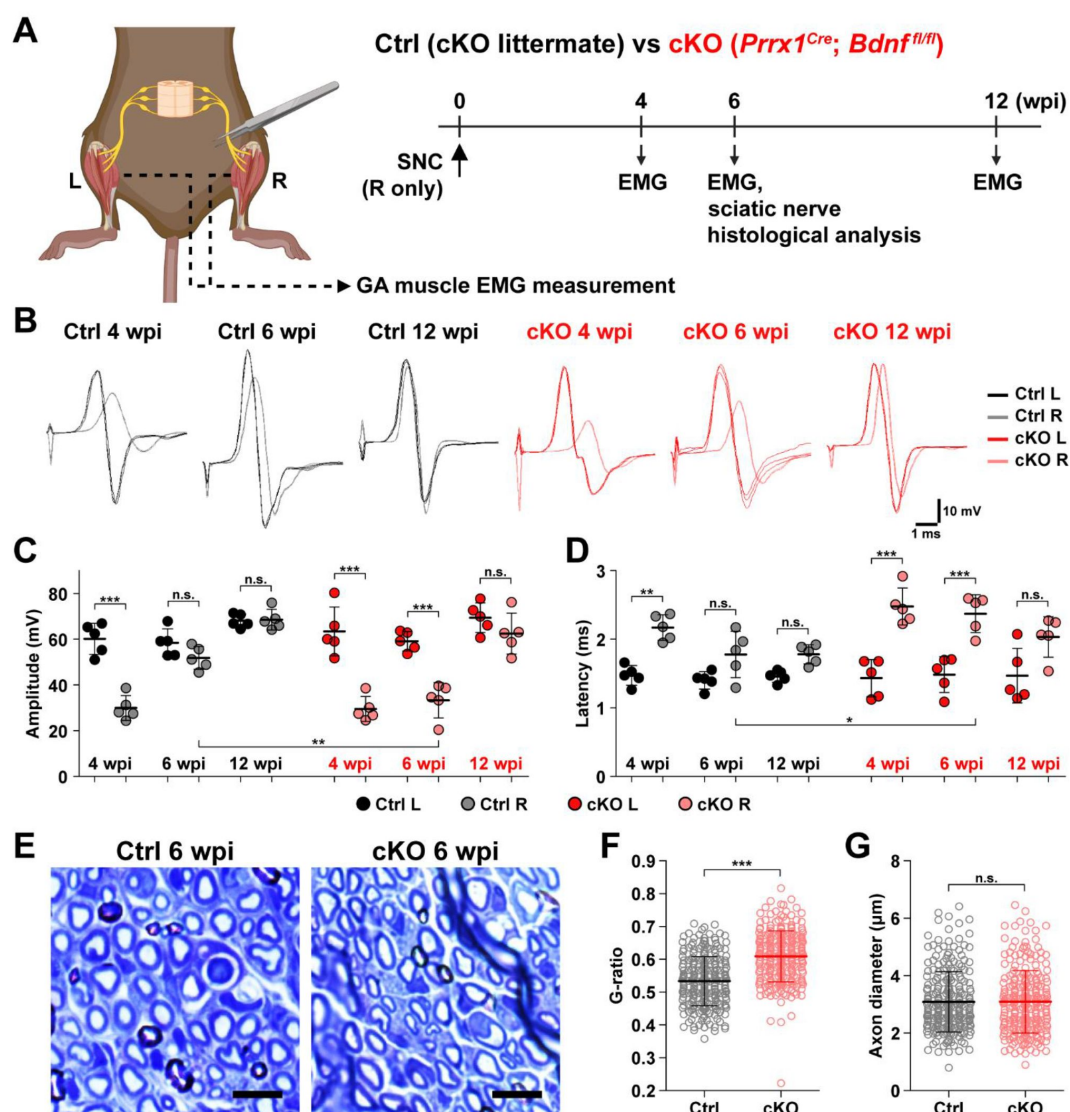


Figure 5.

Remyelination by FAP-derived BDNF during peripheral nerve regeneration.

(A) Experimental scheme displaying mice used and the time points selected for EMG measurements and sciatic nerve dissection. wpi, weeks post injury. See [Figure 5—figure supplement 1D](#) for the EMG measurement scheme. (B) Representative EMG measurement results of both injured and uninjured GA muscles from Ctrl or cKO mice at the indicated time points post SNC. (C–D) Quantified results of EMG measurement showing (C) CMAP amplitude and (D) CMAP latency. $n = 5$. One-way ANOVA with Bonferroni's post hoc test. * $p < 0.05$, ** $p < 0.01$, *** $p < 0.001$, n.s., not significant. See [Figure 5—figure supplement 1E](#) for the EMG measurement quantification methodology. (E) Representative images showing toluidine blue-stained, semi-thin cross-sections of sciatic nerves dissected from Ctrl or cKO mice at 6 wpi. Scale bars, 10 μm. (F–G) Quantification of (F) calculated G-ratio values and (G) axon diameters from analyzing toluidine blue-stained sciatic nerve sections dissected from Ctrl or cKO mice at 6 wpi. 50 axons were randomly selected from each sciatic nerve for quantification. $n = 5$. Mann-Whitney U test. *** $p < 0.001$, n.s., not significant. See [Figure 5—figure supplement 1F](#) and [G](#) for G-ratio quantification scheme and methodology.

© 2024, BioRender Inc. Any parts of this image created with [BioRender](#) are not made available under the same license as the Reviewed Preprint, and are © 2024, BioRender Inc.

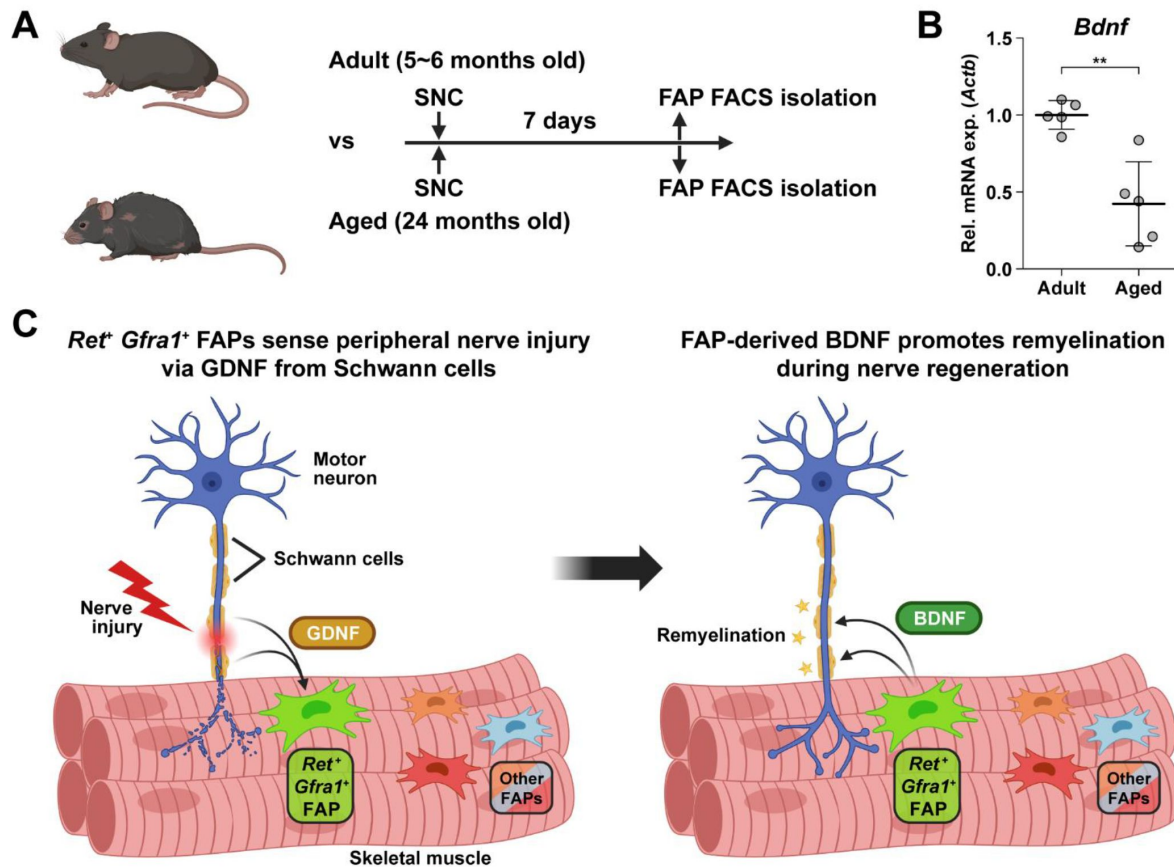


Figure 6.

Implication of FAP-derived BDNF in the age-related delay in nerve regeneration.

(A) Experimental scheme indicating ages of mice used and the time point for FAP isolation to compare the expression level of *Bdnf* post SNC. (B) RT-qPCR results showing the expression level of *Bdnf* in FAPs isolated from either adult (5-6 months) or aged (24 months) mice at 7 dpi. $n = 5$. Unpaired t-test. $** p < 0.01$. (C) Graphical summary of this study.

© 2024, BioRender Inc. Any parts of this image created with BioRender are not made available under the same license as the Reviewed Preprint, and are © 2024, BioRender Inc.

injury had previously been recognized (Hammarberg et al., 1996 [DOI](#); Hoke et al., 2002 [DOI](#); Arthur-Farraj et al., 2012 [DOI](#); Xu et al., 2013 [DOI](#); Proietti et al., 2021 [DOI](#)), we identified FAPs as a major target cell population of GDNF within skeletal muscle, based on the enriched expression of GDNF receptors. In depth, exploiting the technical advantage of scRNA-seq, we suggested that a subset of FAPs, named cluster 1 in this study, can sense the local GDNF by expressing GDNF receptors *Ret* and *Gfra1*, and that upon GDNF sensing, cluster 1 FAPs turn into clusters 2 and 3 to contribute to the nerve regeneration process. Specifically, we discovered that FAPs, especially the *F2rl1*-expressing cluster 2, express *Bdnf* in response to nerve injury and/or GDNF, which in turn was shown to promote the remyelination process by Schwann cells during nerve regeneration, using our cKO mouse model (**Figure 6C** [DOI](#)). Since epineurial and perineurial, but not endoneurial mesenchymal cells share their origins with the muscle-resident FAPs and therefore are *Prrx1*-positive (Joseph et al., 2004 [DOI](#); Carr et al., 2019 [DOI](#)), the possibility that the delayed remyelination observed in our cKO mice could be due to the combined effect of *Bdnf* depletion in both muscle- and nerve-resident mesenchymal cells cannot be eliminated. To resolve such issue, further investigations using muscle-resident FAP-specific Cre mouse lines is required, but such line is currently unavailable as no such specific marker has been found. Nevertheless, our findings show that muscle-resident FAP-derived BDNF is indeed important for nerve regeneration, since intramuscular injection of recombinant BDNF can sufficiently accelerate the nerve regeneration process (Zheng et al., 2016 [DOI](#)). Conversely, intramuscular injection of BDNF-neutralizing antibodies can sufficiently delay nerve regeneration (Zheng et al., 2016 [DOI](#)). Thus, endogenous supply of intramuscular BDNF by the muscle-resident FAPs in our Ctrl mice would likely have supported remyelination by Schwann cells, while the lack of such BDNF supply by FAPs in our cKO mice would have resulted in delayed remyelination. Also, we found that while muscle-resident FAPs robustly express both GDNF receptor genes, neither epineurial nor perineurial mesenchymal cells express significant levels of *Ret* and *Gfra1* (Carr et al., 2019 [DOI](#); Toma et al., 2020 [DOI](#); Zhao et al., 2022 [DOI](#)) (**Supplemental figure 1** [DOI](#)), implying that the GDNF-BDNF axis found in this study could be valid uniquely in muscle-resident FAPs. Collectively, we suggest that muscle-resident mesenchymal progenitors can directly contribute to nerve regeneration via the GDNF-BDNF axis (**Figure 6C** [DOI](#)), of which was previously unidentified; we suggest that in future studies regarding peripheral nerve regeneration, active participation of this intramuscular mesenchymal population should be taken into consideration. In that process, our scRNA-seq data may provide valuable insights, which may lead to additional discoveries on FAP's contributions to nerve regeneration by other mechanisms, and/or provide clues on the cell-to-cell communications of FAPs with other cell types that may lead to facilitation of the regeneration process.

Here, we have primarily investigated the roles of *Ret*-expressing and *F2rl1*-expressing FAPs in sensing and responding to nerve injury, respectively. However, possibilities that other subpopulations can exert distinct beneficial effects on nerve regeneration remain largely unexplored. For example, although identified as a nerve injury-relevant subpopulation in this study, specific contributions of the *Alkal2*-expressing cluster 3 FAPs to nerve regeneration are yet to be discovered. Identification of effector genes such as *Bdnf* from this subpopulation may lead to the discovery of an additional mechanism by which FAPs can contribute to nerve regeneration. Although other subpopulations (clusters 4-7) did not exhibit dramatic fluctuations in population percentage, some of the genes expressed specifically in those subpopulations showed patterns that followed the regeneration process (**Supplemental figure 2** [DOI](#)). Such gene expression patterns suggest subpopulation-specific functions even in the less dynamic subpopulations within FAPs in peripheral nerve regeneration, and require further investigations to reveal their possible contributions.

The role of BDNF in peripheral nerve regeneration has been identified previously, where it was found to promote both intrinsic axonal regeneration in neurons as well as remyelination by Schwann cells (Zhang et al., 2000 [DOI](#); Chan et al., 2001 [DOI](#); Zheng et al., 2016 [DOI](#)). In such circumstances, various cellular sources of BDNF have been identified. Bone marrow transplantation of wild-type cells into *Bdnf* heterozygotic knockout mice revealed the involvement

of bone marrow-derived cells in expressing *Bdnf* that can promote nerve regeneration in the sciatic nerve (Takemura et al., 2012 [DOI](#)). Schwann cells themselves are cellular sources of BDNF during nerve regeneration (Wilhelm et al., 2012 [DOI](#)). In this study, we showed that BDNF from FAPs can also promote myelination of the regenerating axons post injury, suggesting FAPs as an additional cellular source of BDNF in peripheral nerve regeneration. The existence of cellular sources of BDNF other than FAPs such as Schwann cells would provide an explanation for the delayed, but not failed, remyelination in our *Bdnf* cKO mice, where complete regeneration had occurred after a sufficient amount of time, despite the lack of *Bdnf* expression in FAPs. Still, ablation of *Bdnf* in FAPs displayed significant delays in the remyelination process during nerve regeneration, suggesting their requirement in the timely regeneration process of injured nerves. Meanwhile, scRNA-seq data of all mononuclear cells from denervated muscles (Nicoletti et al., 2023 [DOI](#)) suggested expression of *Bdnf* in tenocytes and pericytes in addition to Schwann cells and FAPs (**Supplemental figures 3A** [DOI](#) and **B** [DOI](#)). Although this may imply the involvement of those cellular components in providing BDNF for nerve regeneration, expression of *Bdnf* in such cells were not altered as significantly in response to nerve injury as in FAPs or Schwann cells (**Supplemental figure 3C** [DOI](#)). Moreover, while *Ret*-expressing FAPs and Schwann cells are known to be in proximity to the NMJ or relevant nerve regeneration sites (Leinroth et al., 2022 [DOI](#)), such locational enrichment of tenocytes and pericytes have not been reported so far. Thus, it is likely that FAPs, together with Schwann cells, are the main sources of BDNF within skeletal muscle that can act in the remyelination process during peripheral nerve regeneration.

Aging is one of the well-known factors that can slow down the nerve regeneration process (Verdú et al., 2008 [DOI](#); Maita et al., 2023 [DOI](#)). Since multiple cell types are known to participate in this process (Scheib and Hoke, 2013 [DOI](#)), determination of the cell types that can cause age-related delays in nerve regeneration is important for the development of therapeutic approaches targeting the relevant cell types. Of note, previous research emphasized the importance of niche factors, rather than the intrinsic regenerative capacity of the injured neurons, in the age-related decline in nerve regeneration (Painter et al., 2014 [DOI](#)). Specifically, inability of Schwann cells to adopt repair cell phenotypes has been pointed out as one of the age-related changes (Painter et al., 2014 [DOI](#); Wagstaff et al., 2021 [DOI](#)). In addition, age-related changes in immune cells, especially macrophages, were suggested as causal factors that delay nerve regeneration (Buttner et al., 2018 [DOI](#)). In particular, chronic inflammatory phenotypes were shown to interfere with the remyelination process by Schwann cells (Buttner et al., 2018 [DOI](#)), and failed macrophage infiltration in the early stages of regeneration resulted in defective Wallerian degeneration and myelin debris clearing (Scheib and Hoke, 2016 [DOI](#)). In addition to the involvement of Schwann cells and immune cells, we have identified muscle-resident FAPs as an additional cellular component that can contribute to nerve regeneration, by promoting remyelination via BDNF secretion. Surprisingly, expression of *Bdnf* by FAPs was significantly reduced in aged mice compared to adult mice, suggesting the clinical relevance of FAP's involvement in the age-related delay in peripheral nerve regeneration. We believe that further studies on age-related changes in FAPs may provide valuable clues to understanding clinical observations from aged individuals, which can lead to development of additional therapeutic strategies that include FAPs as target cells in treating both young and aged nerve injury patients.

Materials and Methods

Animals

C57BL/6J (RRID:IMSR_JAX:000664), *Prrx1*^{Cre} (RRID:IMSR_JAX:005584), *Bdnf*^{fl} (RRID:IMSR_JAX:004339), *Plp1*^{CreER} (RRID:IMSR_JAX:005975) and *Rosa*^{tdTomato} (RRID:IMSR_JAX:007914) mice were all obtained from The Jackson Laboratory. To generate *Prrx1*^{Cre}, *Bdnf*^{fl/fl} mice, *Prrx1*^{Cre/+}; *Bdnf*^{fl/+} males and *Bdnf*^{fl/fl} females were crossed to avoid germline recombination in the female reproductive cells, and littermates were used as controls. To

generate *Plp1^{CreER}; Rosa^{tdTomato}* mice, *Plp1^{CreER/+}* mice were crossed with *Rosa^{tdTomato/+}* mice, and the line was kept by breeding *Plp1^{CreER/+}; Rosa^{tdTomato/tdTomato}* males and females. Only mice that had the *Plp1^{CreER}* allele was used. Primers used for genotyping are listed in **Supplemental table 4** [↗](#). All mice were bred on the B6 background, except for the *Prrx1^{Cre}; Bdnf^{fl/fl}* mice and littermates that were kept in the mixed B6, 129S4 and BALB/c background. All mice were housed in a specific-pathogen-free (SPF) animal facility, with 12-h light/12-h dark cycle at room temperature (RT, 22°C) and 40~60% humidity, and were fed with normal chow diet and water ad libitum. Tamoxifen administration, sciatic nerve crush injury, denervation, and intramuscular injection of GDNF or GDNF blocking antibodies were all given to 3 to 4-month-old adult mice. When comparing aged mice versus adult mice, 24-month-old and 5 to 6-month-old mice were used, respectively. In all cases except for *Plp1^{CreER}; Rosa^{tdTomato}* mice, male mice were used for the experiments. No sex-specific differences were observed in experiments using *Plp1^{CreER}; Rosa^{tdTomato}* mice. All experimental procedures were approved by the Institutional Animal Care and Use Committee at Seoul National University and were carried out according to the guidelines provided.

Tamoxifen administration

To label Schwann cells, 3-month-old *Plp1^{CreER}; Rosa^{tdTomato}* mice were administered orally with tamoxifen (20 mg/ml in corn oil, 160 mg/kg body weight; Sigma-Aldrich) 3 times every other day.

Sciatic nerve injury

Mice were deeply anesthetized via intraperitoneal injection of Avertin (32 mg/ml, ~800 mg/kg; Sigma-Aldrich), and the incision site on the posterior side of the right hindlimb was shaved and depilated using surgical clippers and hair removal cream. After cleansing the incision site with 70% ethanol, incision was made on the skin with surgical scissors and the biceps femoris muscle was punctured open with fine-tip forceps to expose the sciatic nerve. For sciatic nerve crush injury, the exposed nerve was crushed with fine forceps for 30 seconds at the site just proximal to where the tibial, peroneal and sural nerves branched out from the sciatic nerve. For denervation, ~5 mm of the sciatic nerve proximal from the crush injury site was cut and removed. The punctured biceps femoris muscle and skin were then sutured, and the incision site was sterilized with povidon-iodine.

Intramuscular injection of GDNF

Tibialis anterior muscle and the two gastrocnemius muscles (GA, lateral and medial) were each injected with 10 µl of either PBS or recombinant mouse GDNF (10 µg/ml, Sigma-Aldrich) using 31-gauge insulin syringes without damaging any innervating nerves. The injected muscles were then dissected 48 hours post injection for isolation of FAPs and further analysis.

Intramuscular injection of GDNF blocking antibodies

Tibialis anterior muscle and the two gastrocnemius muscles (GA, lateral and medial) were each injected with 10 µg of either normal rabbit IgG (Sino Biological) or anti-GDNF antibodies (Alomone Labs) using 31-gauge insulin syringes 24 hours post SNC. The injected muscles were then dissected 48 hours post injection (72 hours post injury) for isolation of FAPs and further analysis.

Isolation of FAPs, Schwann cells and others

Isolation of muscle-resident FAPs, Schwann cells and others was performed according to a previously reported protocol ([Liu et al., 2015](#) [↗](#)) with minor modifications. Muscles indicated in each experiment were dissected, finely chopped with surgical scissors and washed with 10% horse serum (Gibco), DMEM (HyClone) for further dissociation. Enzymatic dissociation was carried out in 10% horse serum, DMEM containing collagenase II (800 U/ml, Worthington Biochemical) and dispase II (1.1 U/ml, Gibco) for 40 minutes at 37°C with mild agitation, and mechanical dissociation

was performed by titration of the dissociated solution with a 20-gauge needle ten times. After filtering the solution through a 40 μm strainer, dissociated mononuclear single cells were stained with the following antibodies: APC anti-mouse CD31, APC anti-mouse CD45, PE anti-mouse TER-119, biotin anti-mouse CD106 (Vcam1) (Biolegend) and FITC anti-mouse Ly-6A/E (Sca1) (BD Pharmingen). 7-aminoactinomycin D (7-AAD, Sigma-Aldrich) was added to stain dead cells, and PE/Cy7 streptavidin was used to label Vcam1⁺ cells. Gating strategies used for the isolation of each cell type were as follows: FAPs, 7-AAD⁻Ter119⁻CD31⁻CD45⁻Vcam1⁺Sca1⁺; MuSCs, 7-AAD⁻Ter119⁻CD31⁻CD45⁻Vcam1⁺Sca1⁻; lineage-positive cells, 7-AAD⁻Ter119⁻CD31⁺ or 7-AAD⁻Ter119⁻CD45⁺; double-negative cells, 7-AAD⁻Ter119⁻CD31⁻CD45⁻Vcam1⁻Sca1⁻. For Schwann cells, 7-AAD⁻tdTomato⁺ cells were sorted from tamoxifen-administered *Plp1^{CreER}; Rosa^{tdTomato}* mice.

scRNA-seq library construction and sequencing

FAPs were isolated from sciatic nerve crush injury-affected or denervated muscles on days 3, 7, 14 and 28 post injury using wild type B6 mice, so that a total of nine samples, including uninjured control, were collected for library generation. For each sample, isolated FAPs were pooled from two mice. Chromium Next GEM Single Cell 3' Kit v3.1 (10x Genomics) was used according to the manufacturer's instructions for the nine collected FAP samples, and target cell number for recovery was set to 5,000 in each sample. Sequencing of the libraries was carried out using HiSeq X Ten (Illumina).

Computational analysis of scRNA-seq data

Sequenced reads were aligned to the mouse reference genome mm10 using CellRanger v3.1.0 (10x Genomics), and aligned reads were transformed into gene-cell count matrices using velocity v0.17 (La Manno et al., 2018 [\[1\]](#)) to obtain count matrices for both spliced and unspliced mRNAs. Output loom files were then loaded with R package SeuratWrappers v0.3.1, and were preprocessed and analyzed using R package Seurat v4.3.0 (Hao et al., 2021 [\[2\]](#)) for downstream analysis. The preprocessing steps for quality control included doublet filtering, live cell filtering and removal of non-FAPs as previously described (Kim et al., 2022 [\[3\]](#)). All nine sample data were merged and normalized for dimensionality reduction, where top 8 principal components from the principal component analysis using 5,000 variable genes were selected for 2-dimensional UMAP embedding and visualization. Unsupervised clustering of cells was achieved through FindNeighbors and FindClusters functions in Seurat R package. To identify DEGs in the pairwise comparisons of scRNA-seq samples, the FindMarkers function in Seurat R package was used with the following parameters: fold change ≥ 2 , pseudocount.use = 0.01, min.pct = 0.01, adjusted p value < 0.05 . For identification of DEGs in each cluster, FindAllMarkers function was used with the parameters: fold change ≥ 1.5 , pseudocount.use = 0.01, min.pct = 0.02, adjusted p value < 0.05 . For hierarchical clustering, R package pheatmap v1.0.12 was used. For RNA velocity analysis, R package velocity v0.6 was used following the instructions provided by the developer (La Manno et al., 2018 [\[1\]](#)). For the prediction of upstream regulatory transcription factors using lists of DEGs enriched in the selected FAP clusters, the web-based tool TRRUST v2 (Han et al., 2018 [\[4\]](#)) was used. For color mapping of the MAPK signaling pathway, online version of the KEGG Mapper – Color (Kanehisa et al., 2023 [\[5\]](#)) was used.

Gene set overrepresentation analysis

To identify pathways enriched in the lists of DEGs, web-based version of g:Profiler (Kolberg et al., 2023 [\[6\]](#)) was used with the following parameters: organism – *Mus musculus*; ordered query – YES; data sources – GO biological process without electronic GO annotations, Reactome, and WikiPathways; advanced options were set to default. Visualization of the results were done as previously described (Reimand et al., 2019 [\[7\]](#)), using the Cytoscape v3.10.1 (Shannon et al., 2003 [\[8\]](#)) application with tools EnrichmentMap v3.3.6 (Merico et al., 2010 [\[9\]](#)) and AutoAnnotate v1.4.1 (Kucera et al., 2016 [\[10\]](#)).

RNA extraction and qRT-PCR

Total RNA extraction and reverse transcription was carried out for isolated FAPs, Schwann cells, MuSCs and others using TRIzol™ reagent (Invitrogen) and ReverTra Ace™ qPCR RT Master Mix (Toyobo) reagents respectively, following the manufacturer's instructions. qPCR was performed using ORA™ SEE qPCR Green ROX L Mix (HighQu) reagent, with gene-specific primers listed in **Supplemental table 4** [↗](#). Quantitative analysis of mRNA levels were done using the $2^{-\Delta\Delta C_t}$ method with β -actin (*Actb*) as the housekeeping gene for normalization.

Western blot analysis

FACS-isolated FAPs were lysed in RIPA buffer (Biosesang) added with 1x Halt protease inhibitor cocktail (Thermo Scientific), and were sonicated. The lysate was then centrifuged at 13,000 rpm for 30 minutes at 4°C, and the supernatant was mixed with Laemmli sample buffer before heating at 95°C for 10 minutes. Samples were subjected to electrophoresis in 10% polyacrylamide gels and transferred to 0.45 μ m PVDF membranes (Immobilon). For GAPDH (rabbit anti-GAPDH, 1:1000, Bethyl Laboratories) and PDGFR α (rabbit anti-PDGFR α , 1:200, Santa Cruz Biotechnology), membranes were blocked in 5% skim milk (LPS Solution), 0.1% Tween-20 (Sigma-Aldrich) in TBS, and incubated with primary antibodies overnight at 4°C, and then with the secondary antibody (horseradish peroxidase-conjugated anti-rabbit IgG, 1:10,000, Promega) for 1 hour at RT. For BDNF (rabbit anti-BDNF, 1:1000, Alomone Labs), membranes were blocked in 5% bovine serum albumin (Bovogen Biologicals), 0.1% Tween-20 in TBS, and incubated with the primary antibody in immunoreaction enhancer solution 1 (Toyobo) for 1 hour at RT, and then with the same secondary antibody in immunoreaction enhancer solution 2 (Toyobo) for 1 hour at RT. The membranes were then developed using SuperSignal West Dura Extended Duration Substrate (Thermo Scientific) according to the manufacturer's instructions, and imaged with FUSION Solo chemiluminescence imaging system (Vilber Lourmat). Densitometric quantification of the imaged data were performed using ImageJ v1.51n (NIH).

Electromyography and CMAP measurement

Intraperitoneal injection of Avertin (32 mg/ml, ~800 mg/kg) for anesthetization of mice was carried out prior to CMAP measurement. Stimulation of the sciatic nerve was achieved by placing stimulating electrodes subcutaneously on either side of the sciatic notch and applying supramaximal stimuli (~70 mA) at a rate of 1 pulse per second with the duration of 0.1 ms, using Isolated Pulse Stimulator Model 2100 (A-M Systems). Recording electrode was placed carefully on the GA muscle subdermally without puncturing the muscle, with the reference electrode placed near the Achilles tendon and ground electrode placed on the tail for data recording using Data Recorder IX-RA-834 (iWorx). CMAP amplitude was determined by the absolute difference between potentials of positive and negative peaks, and CMAP latency was determined by the delay from stimulus peak to the beginning of response peak. Three individual measurements were taken from each animal's GA muscle, and average values were used as representatives for statistical analysis.

Toluidine blue staining of sciatic nerves

Sciatic nerve distal to the injury site was dissected at 6 weeks post injury for analysis. The dissected nerves were fixed in 4% paraformaldehyde dissolved in Sorensen's phosphate buffer (0.1M, pH 7.2) at 4°C overnight, followed by procedures described previously (Kim et al., 2022 [↗](#)) with minor modifications for semi-thin sectioning. Briefly, fixed samples were washed with 0.1M sodium cacodylate buffer (pH 7.2), post-fixed with 1% osmium tetroxide in 0.1M sodium cacodylate buffer (pH 7.2) for 1 hour at RT, washed with distilled water (DW) and stained with 0.5% uranyl acetate at 4°C overnight. Stained samples were then washed with DW and dehydrated using serial ethanol and propylene oxide. Samples were then embedded in Spurr's resin (Electron Microscopy Sciences), and semi-thin sections (500 nm) were prepared with a diamond knife on an ultramicrotome EM UC7 (Leica). The sections were dried down on glass slides for staining and light

microscopy. Toluidine blue staining were done using 1% toluidine blue solution containing 1% sodium borate on a slide warmer (70°C), and images were obtained with the light microscope EVOS FL Auto 2 (Thermo Fisher Scientific) for analysis.

G-ratio quantification

Semi-automated quantification of naked and myelinated axon diameters were carried out using an ImageJ plugin for g-ratio quantification (Goebbels et al., 2010 [DOI](#)), where axon diameters and G-ratios were quantified and calculated, respectively. G-ratios were calculated as [naked axon diameter]/[myelinated axon diameter].

Quantification and statistical analysis

All statistical analyses were performed using Prism v5.01 (GraphPad) and R v4.2.1. Continuous variables were tested for normal distribution with Shapiro-Wilk test, and F-test was used to check for equal variance. For comparison of significant differences in multiple groups, one-way analysis of variance (ANOVA) followed by Bonferroni's pairwise post hoc test was applied. For comparison of two groups, unpaired t-test was used for data with normal distribution and equal variance; Welch's t-test was used for data with normal distribution and unequal variance; and Mann-Whitney U test was used for non-normally distributed data. ANCOVA was applied to test for differences between slopes of linear regression lines. Two-way ANOVA was applied to compare two groups with two variables. For comparison of gene expression levels between scRNA-seq data, Wilcoxon rank sum test was applied as a default in functions FindAllMarkers and FindMarkers within the R package Seurat v4.3.0. For RT-qPCR, the average of triplicate technical values were used for each biological replicate. All error bars represent mean \pm SD. *P* value of less than 0.05 was considered statistically significant at the 95% confidence level. The number of technical and biological replicates and statistical analysis used in each experiment are indicated in the figure legends.

Data availability

Single-cell RNA-sequencing data produced in this study have been deposited at GEO under accession number GSE250436 and are publicly available as of the date of publication.

Acknowledgements

We thank Dr. Jong-Eun Park for his helpful comments on the analysis of our scRNA-seq data. *Prrx1^{Cre}* mice, *Bdnf^{fl}* mice, and *Plp1^{CreER}* mice were obtained via Korea Mouse Phenotyping Center, deposited by Dr. Rho Hyun Seong, Dr. Yun-Hee Lee, and Dr. Myunghwan Choi, respectively. Also, we would like to acknowledge technical support from Center for Research Facilities, Biological Sciences Department, Seoul National University (SNU) and SNU National Instrumentation Center for Environmental Management. Library construction and sequencing of the scRNA-seq data was performed by Macrogen Inc.. Experimental schemes and graphical summary in this paper were created using BioRender. This work was supported by grants from the National Research Foundation of Korea (NRF-2020R1A5A1018081, NRF-2022R1A2C3007621) funded by the Korean government (MSIT).

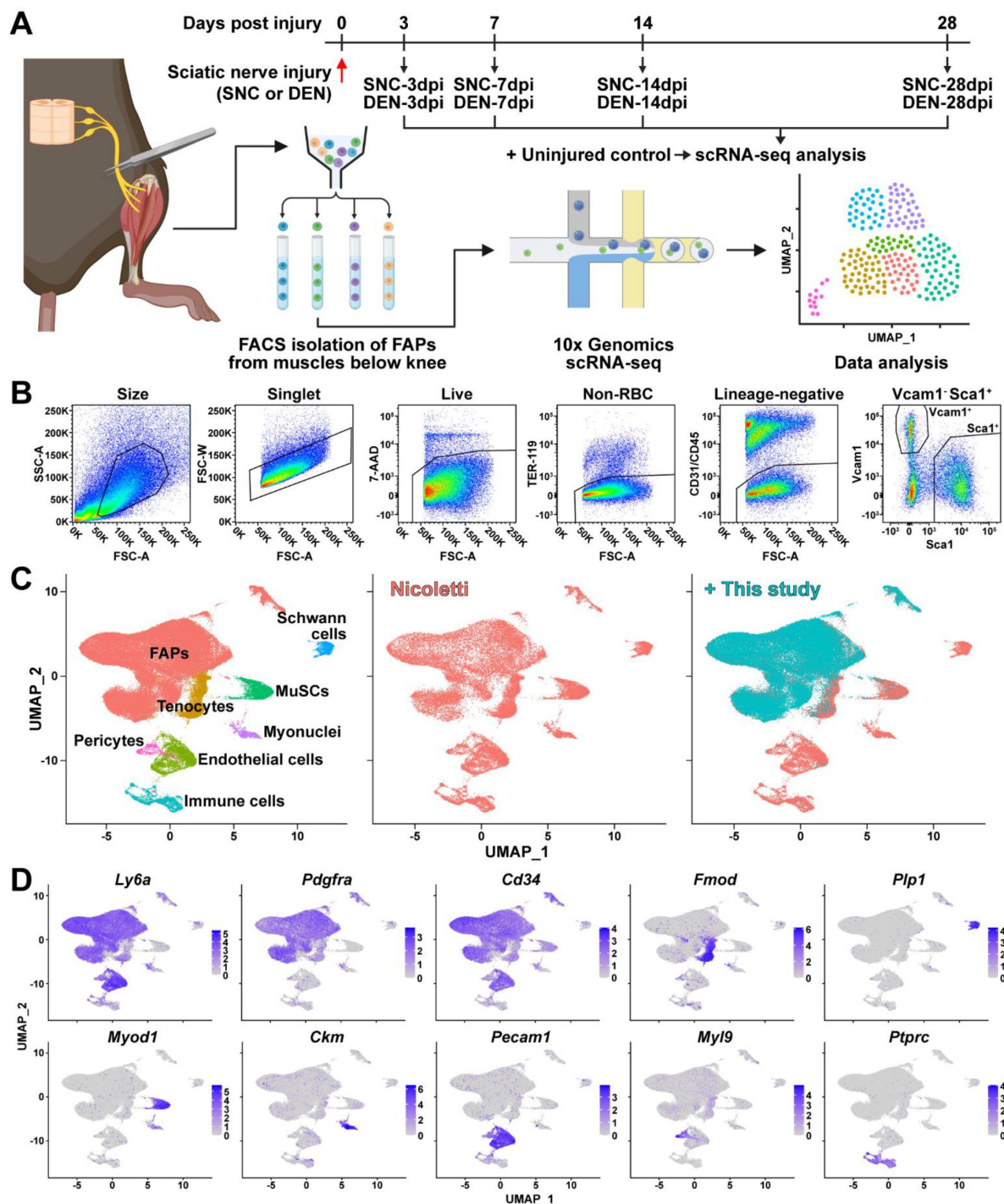


Figure 1—figure supplement 1.

Establishment and validation of nerve injury-affected FAPs' scRNA-seq data.

(A) Experimental scheme depicting the procedures for sample collection and scRNA-seq. The types of nerve injuries and time points for FAP isolation for each sample are specified. (B) Gating strategies used for FACS isolation of FAPs. (C) Integration of scRNA-seq data obtained in this study and data from Nicoletti et al. (2023) visualized on UMAP plots. Left: integrated data labeled with cell types; middle: cells from Nicoletti et al. (2023) only; right: data from this study overlaid on top of data from Nicoletti et al. (2023). (D) Expressions of marker genes that distinguish cell types within skeletal muscle in the integrated scRNA-seq data visualized on UMAP plots.

© 2024, BioRender Inc. Any parts of this image created with BioRender are not made available under the same license as the Reviewed Preprint, and are © 2024, BioRender Inc.

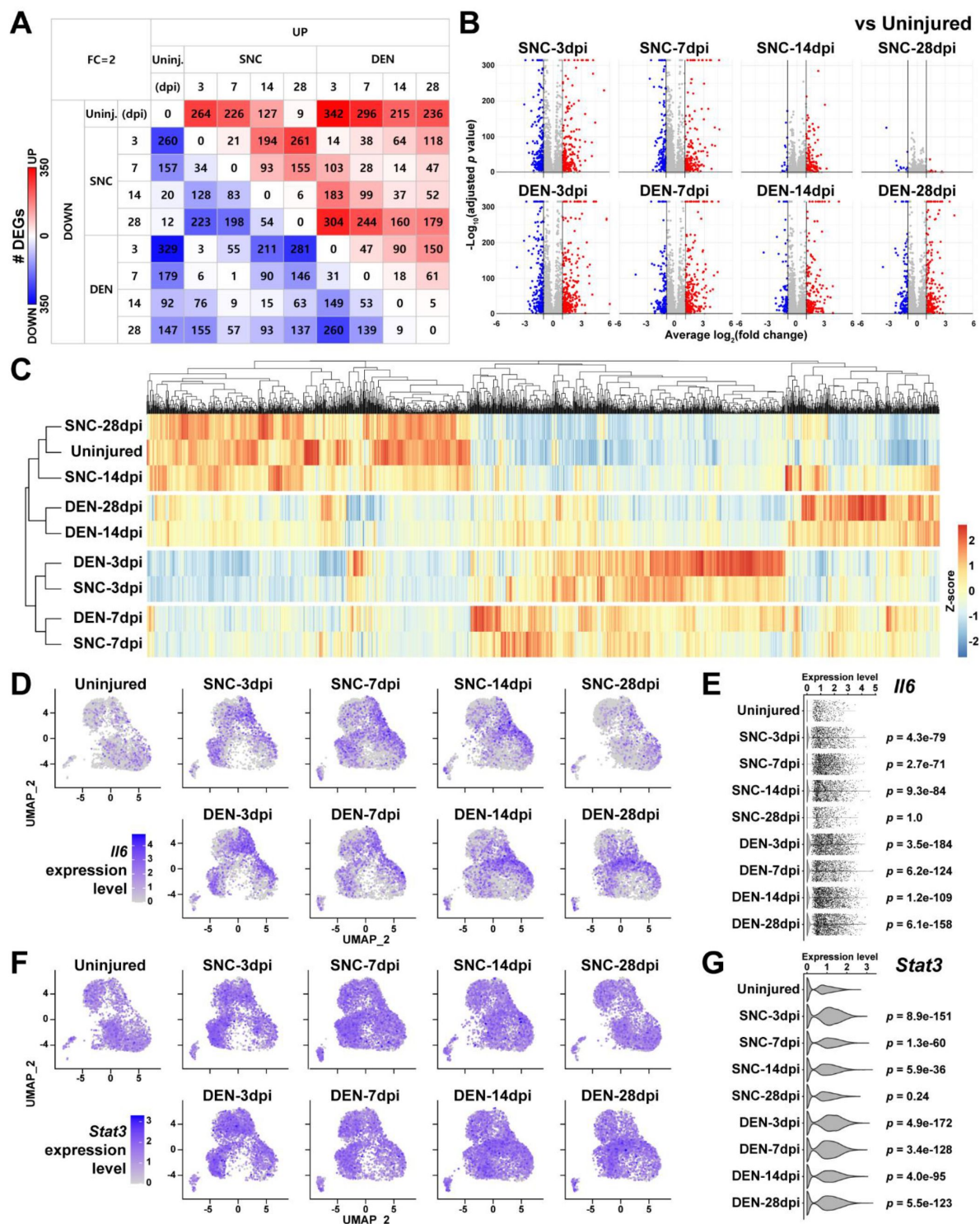


Figure 1—figure supplement 2.

DEG analyses reveal similarities and differences between FAPs affected by SNC or DEN at different time points.

(A) Number of DEGs identified from pairwise comparisons of all nine scRNA-seq samples visualized as a heatmap. (B) DEGs identified from comparing nerve injury-affected FAPs versus uninjured control shown on volcano plots. (C) Hierarchical clustering of the nine scRNA-seq samples using DEGs identified in (A) displayed as a heatmap. (D and F) UMAP plots showing the expressions of (D) *Il6* and (F) *Stat3*. (E and G) Violin plots showing the expressions of (E) *Il6* and (G) *Stat3*, with p values calculated from comparing each sample to uninjured control. Wilcoxon rank sum test.

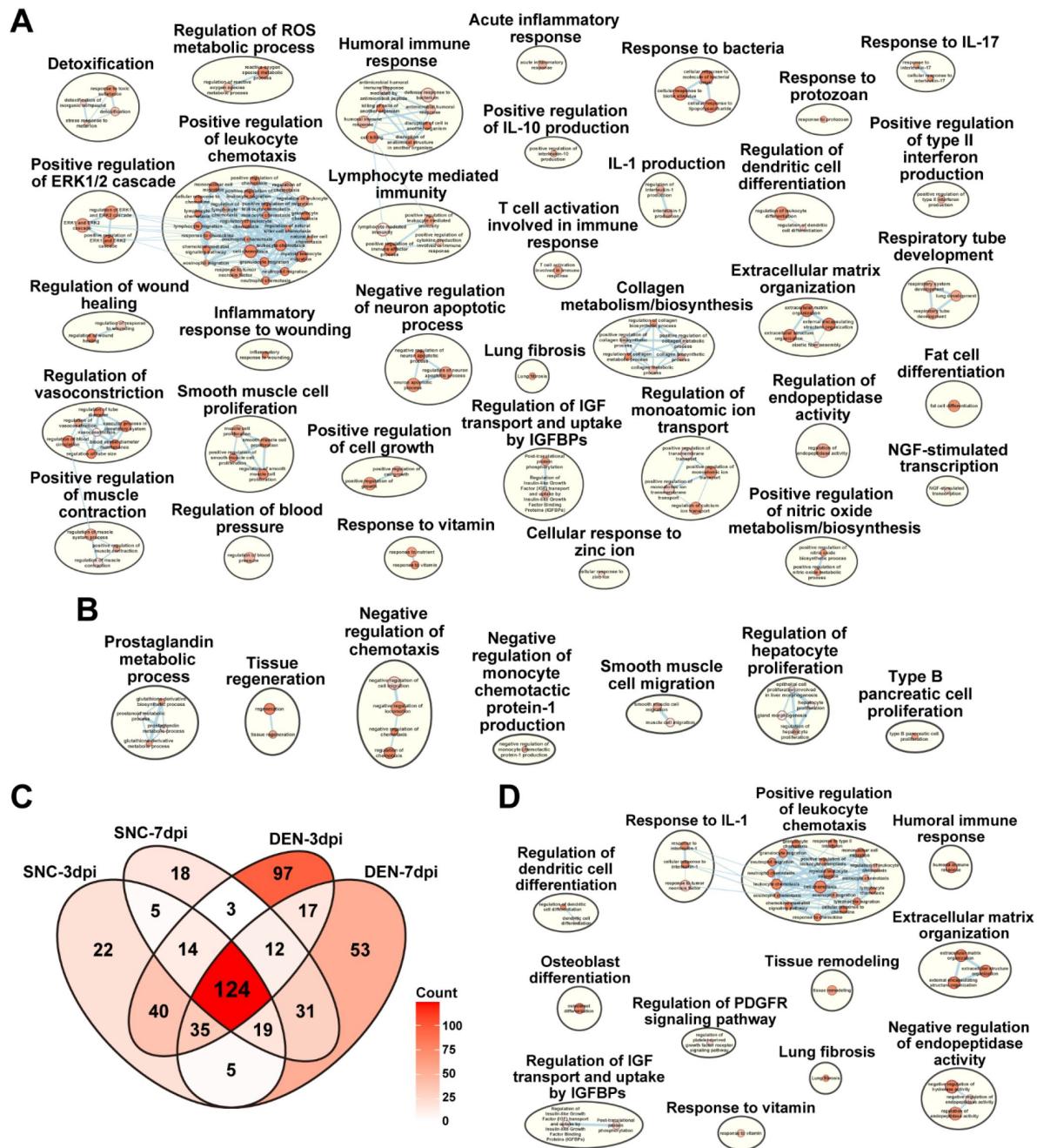


Figure 1—figure supplement 3.

Gene set overrepresentation analyses using DEGs from pairwise comparisons of the nine scRNA-seq samples.

(A–B) Results from g:Profiler showing pathways enriched using DEGs upregulated in (A) DEN-28dpi versus SNC-28dpi and (B) vice versa. (C) Venn diagram showing the number of overlapping genes identified as DEGs by comparing each indicated sample to uninjured control. (D) Results from g:Profiler showing pathways enriched using DEGs shared in all four samples compared to uninjured control, as shown in (C).

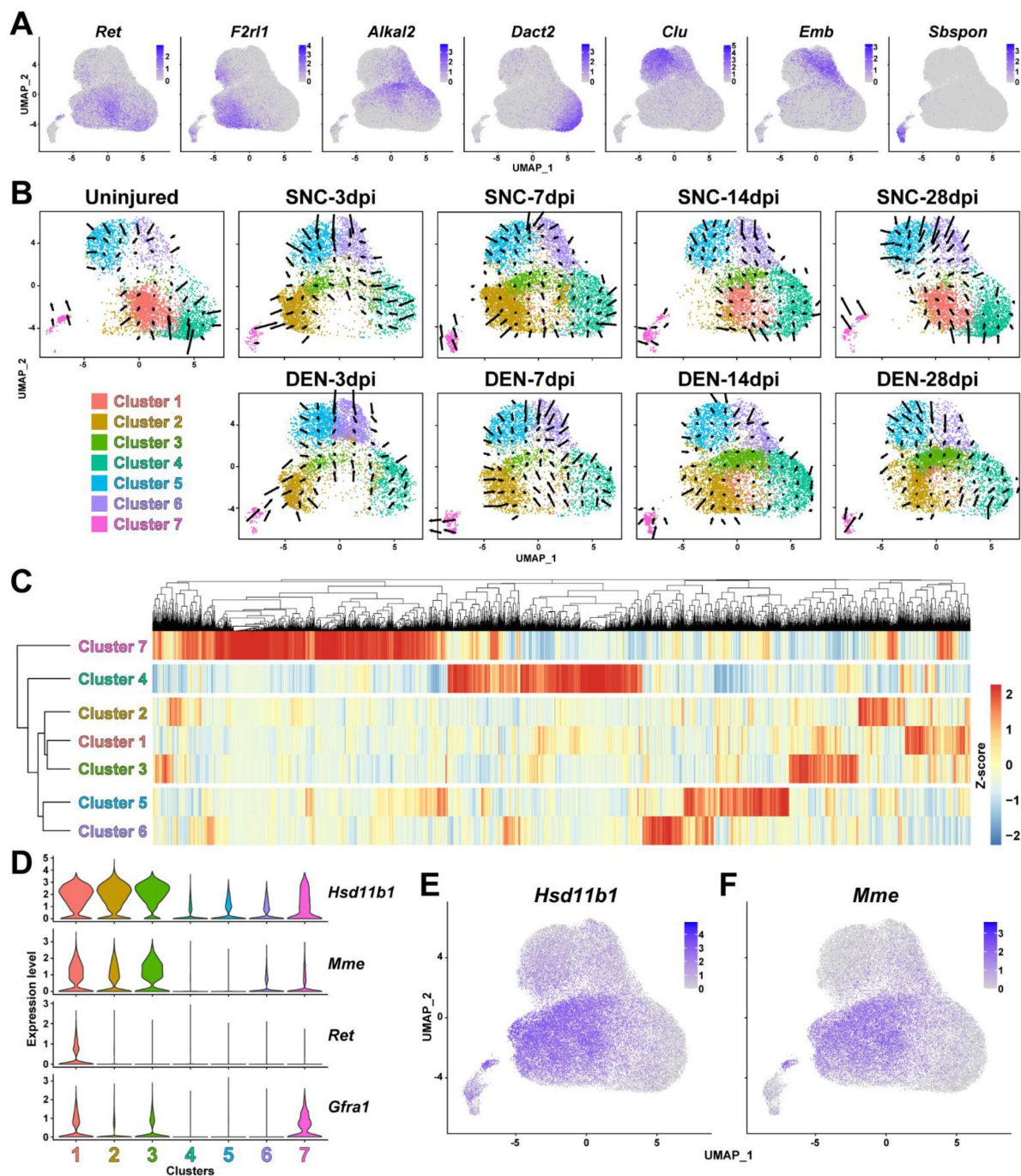


Figure 2—figure supplement 1.

Identification of FAP clusters that respond to nerve injury.

(A) UMAP plots showing expressions of cluster-specific marker genes identified in this study. (B) Results from RNA velocity analysis visualized on UMAP plots. Arrows indicate the predicted direction of cellular movement in the near future on the UMAP plots. (C) Hierarchical clustering of the seven FAP clusters displayed with a heatmap. (D) Violin plots showing the expressions of marker genes previously reported by Leinroth et al. (2022) in the seven clusters identified in this study. (E–F) Expressions of (E) *Hsd11b1* and (F) *Mme* shown on UMAP plots.

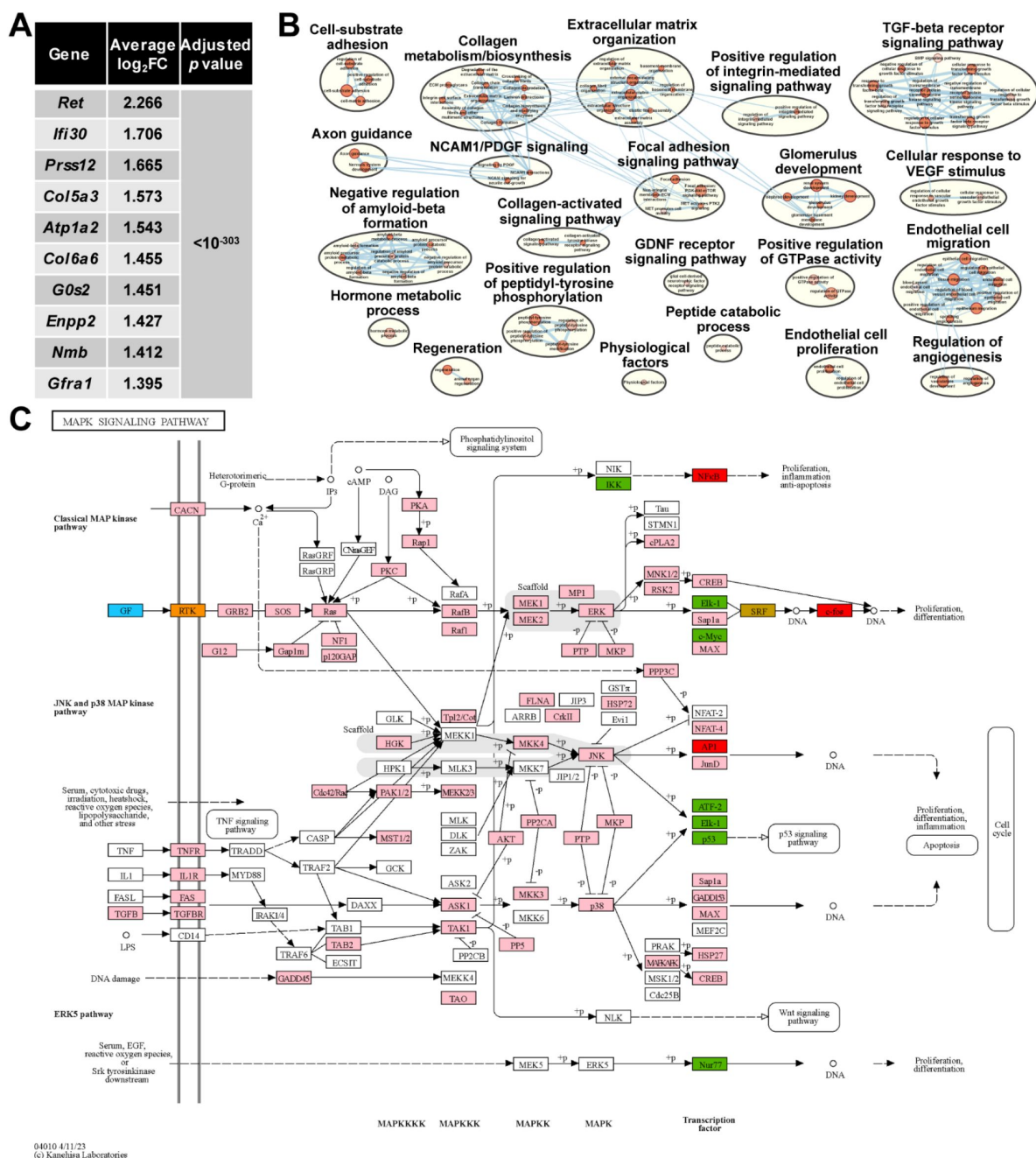


Figure 3—figure supplement 1.

Involvement of GDNF signaling pathway in the nerve injury-sensing mechanism by cluster 1 FAPs.

(A) Top 10 genes specifically enriched in cluster 1 FAPs. *P* values were drawn from Wilcoxon rank sum test.

(B) Results from g:Profiler showing pathways enriched using genes specifically enriched in cluster 1. (C) MAPK signaling pathway retrieved from KEGG, with color-coding to highlight relevant genes. Blue: GDNF ligand; orange: GDNF receptor RET expressed in cluster 1; pink: downstream cascade genes expressed in clusters 1-3; red: transcription factors (TFs) commonly predicted to regulate upregulated genes in clusters 2 and 3; green: TFs predicted to regulate genes upregulated in cluster 2; gold: TFs predicted to regulate genes upregulated in cluster 3.

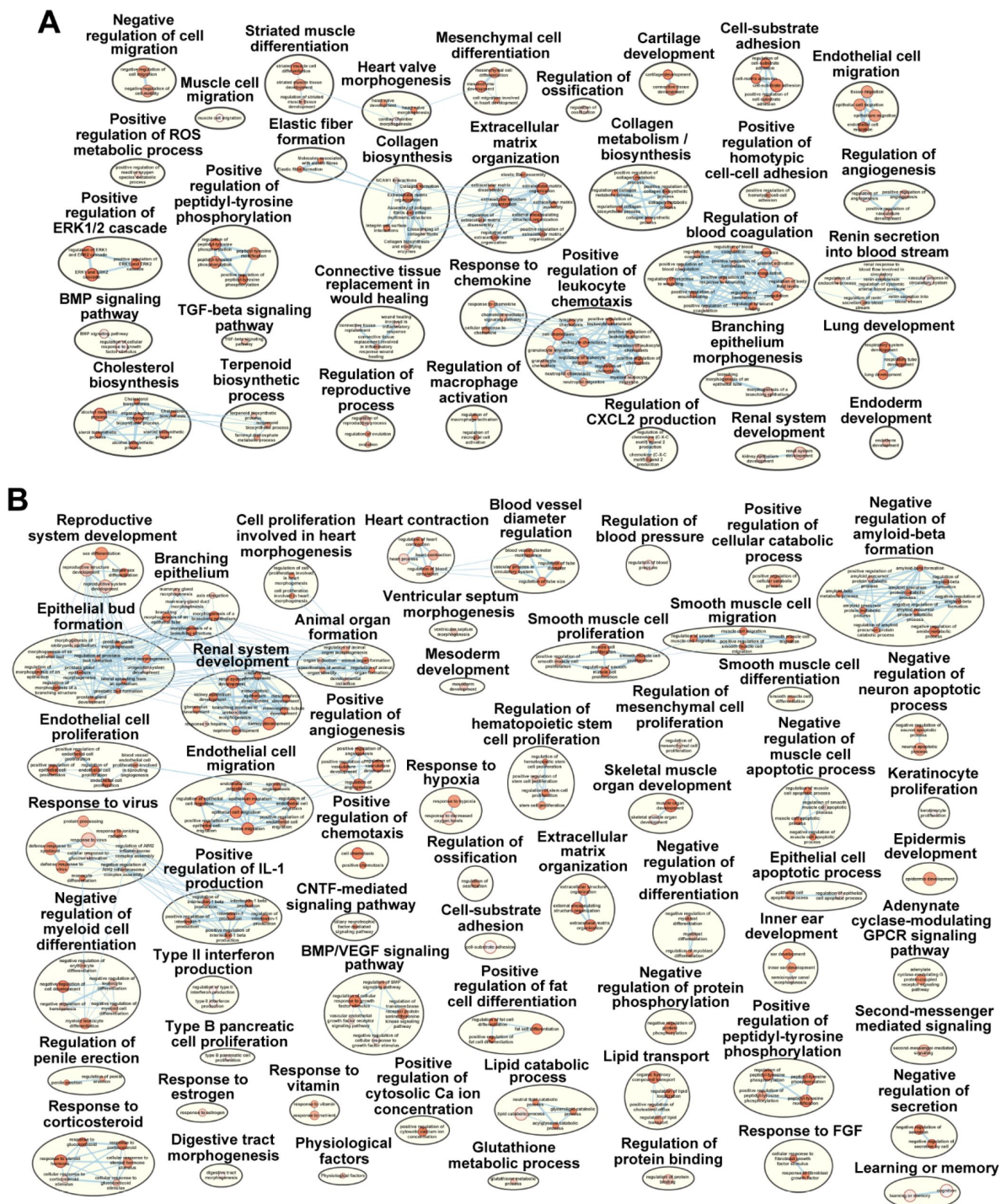


Figure 3—figure supplement 2.

Pathways enriched in the two activated clusters within nerve injury-affected FAPs.

(A–B) Results from g:Profiler showing pathways enriched using genes specifically enriched in (A) cluster 2 or (B) cluster 3.

Figure 4—figure supplement 1.

Scheme for western blot analysis.

Experimental scheme depicting sample collection for FAP isolation and the timeline for SNC and FAP isolation for the western blot analysis done in **Figure 4F**.

© 2024, BioRender Inc. Any parts of this image created with *BioRender* are not made available under the same license as the Reviewed Preprint, and are © 2024, BioRender Inc.

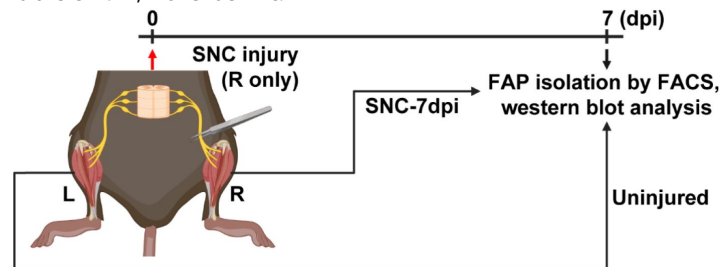
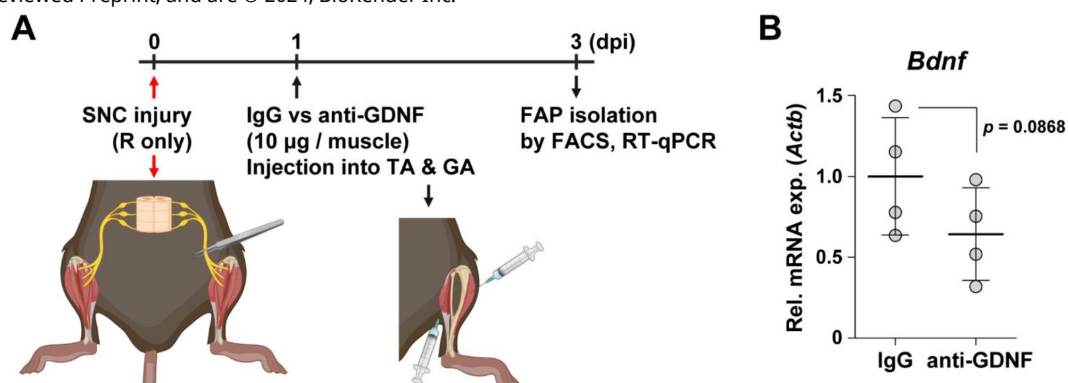


Figure 4—figure supplement 2.

Decreased intramuscular GDNF activity can weaken *Bdnf* induction in FAPs upon nerve injury.

(A) Experimental scheme depicting intramuscular injection of either anti-GDNF antibodies or IgG control after SNC, along with the experimental timeline. (B) RT-qPCR results showing the expression levels of *Bdnf* in nerve injury-exposed FAPs affected by intramuscular injection of either IgG control or anti-GDNF antibodies. $n = 4$. Unpaired t-test.

© 2024, BioRender Inc. Any parts of this image created with *BioRender* are not made available under the same license as the Reviewed Preprint, and are © 2024, BioRender Inc.



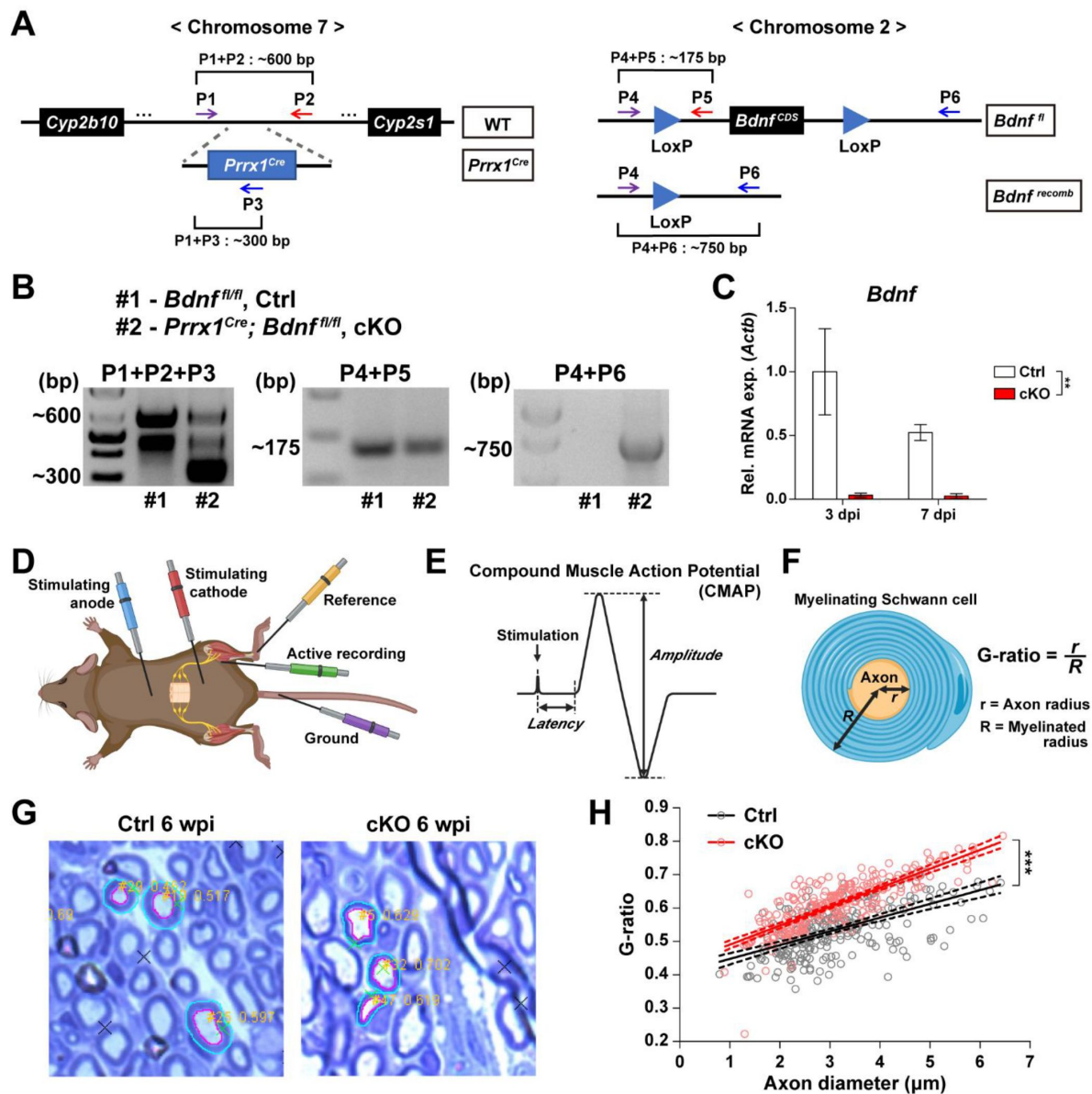
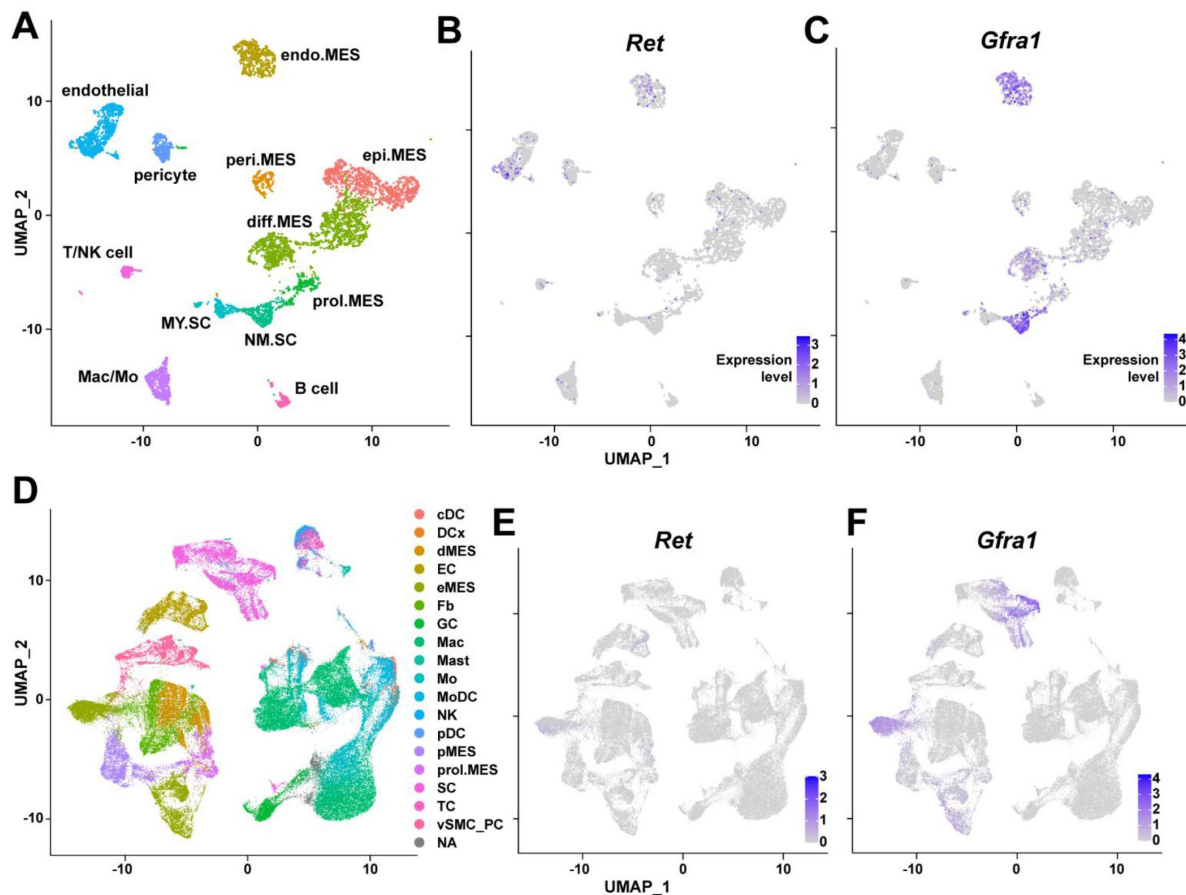


Figure 5—figure supplement 1.

Validation of cKO mice used in this study and methods used for analysis.

(A) Genomic loci and structure of *Prrx1^{Cre}* and *Bdnf^{fl/fl}* alleles labeled with primers used for genotyping and genomic DNA recombination validation. (B) Results from genotyping (left and middle) and genomic DNA recombination PCR (right). Genomic DNA recombination of the LoxP flanking sites in the cKO mice were confirmed using primers P4 and P6 shown in (A). (C) RT-qPCR results of *Bdnf* expression using FAPs isolated from either Ctrl or cKO mice at 3 or 7 days post-SNC. n = 2; Two-way ANOVA. ** $p < 0.01$. (D) Scheme for CMAP measurement showing the positions of electrodes used. (E) Diagram of a typical CMAP graph along with amplitude and latency used for analysis. (F) Diagram depicting calculation of G-ratio. (G) Examples of images from G-ratio quantification using ImageJ plugin GRatio for ImageJ. (H) Scatter plots with linear regressions displaying G-ratios (y-axis) in relation to axon diameters (x-axis). Solid lines are linear regressions and dotted lines represent error in 95% confidence level. ANCOVA, *** $p < 0.001$.

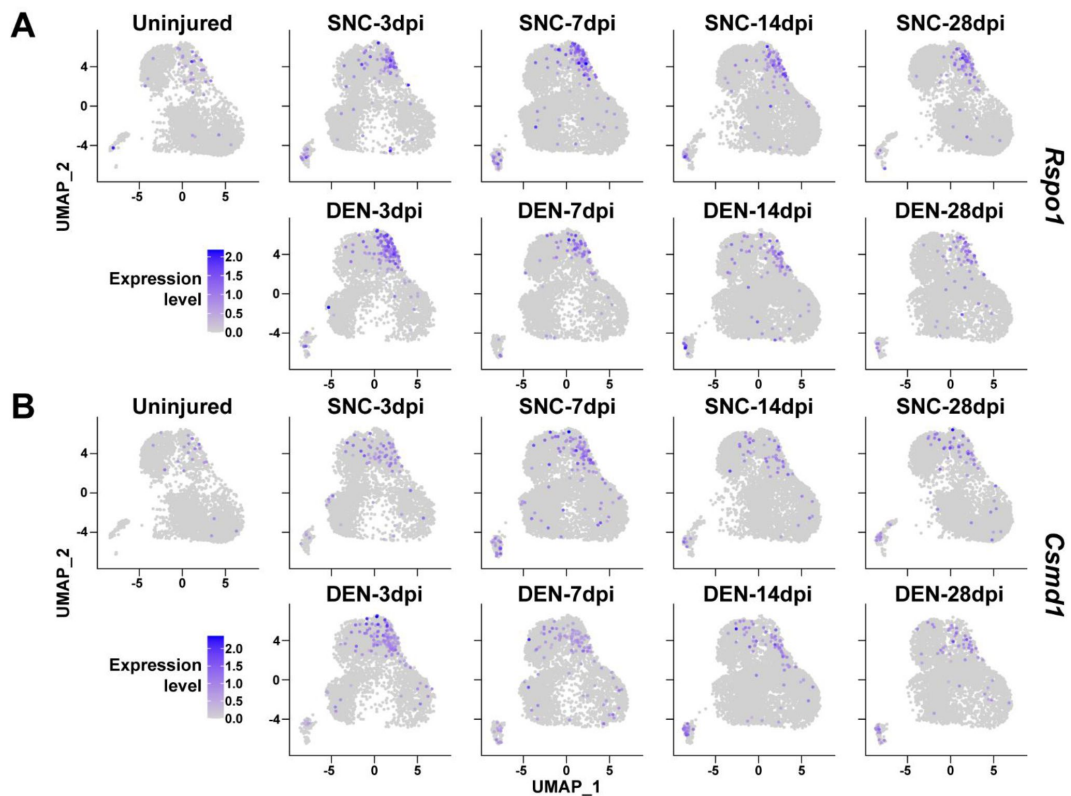
© 2024, BioRender Inc. Any parts of this image created with BioRender are not made available under the same license as the Reviewed Preprint, and are © 2024, BioRender Inc.



Supplemental figure 1.

Expression of GDNF receptor genes *Ret* and *Gfra1* in nerve-resident cells.

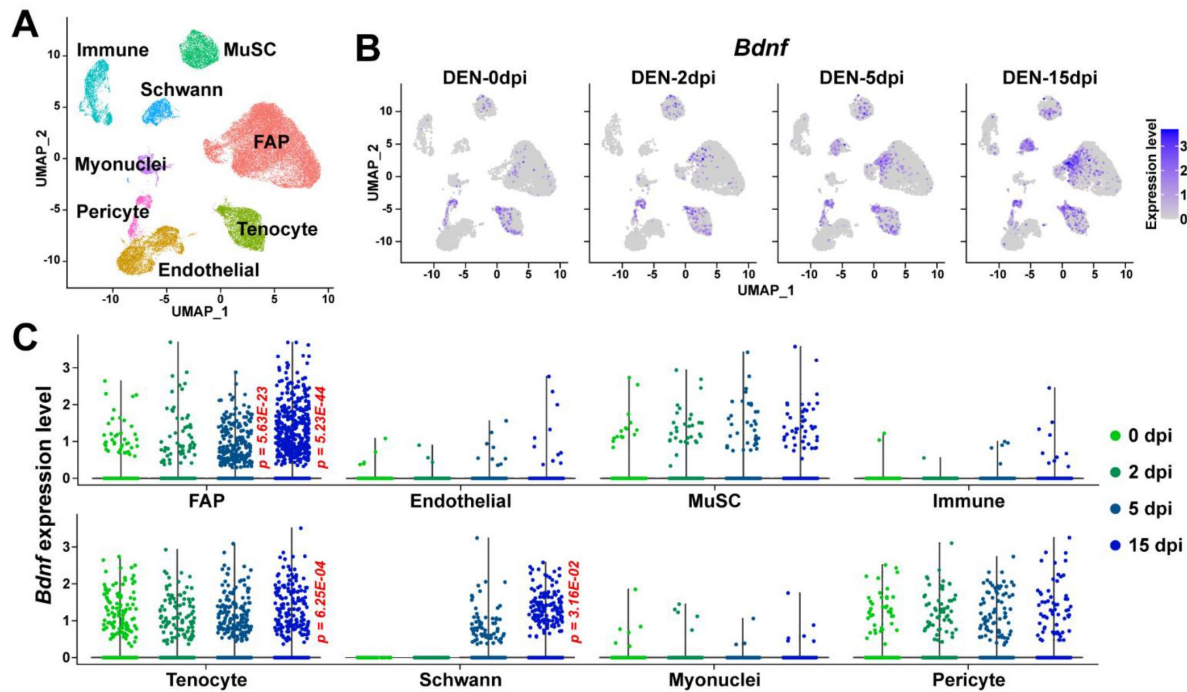
(A–C) scRNA-seq data from Carr et al. (2019) [\[1\]](#) and Toma et al. (2020) [\[2\]](#) (accession numbers: GSM3408137, GSM3408139, GSM4423509, and GSM4423506) were merged into a single Seurat object and visualized on UMAP plots. Cell types identified using markers listed by Toma et al. (2020) [\[2\]](#) are shown in (A), and expression levels of (B) *Ret* and (C) *Gfra1* are displayed. epi.MES: epineurial mesenchymal cells; peri.MES: perineurial mesenchymal cells; endo.MES: endoneurial mesenchymal cells; diff.MES: differentiating mesenchymal cells; prol.MES: proliferating mesenchymal cells; NM.SC: non-myelinating Schwann cells; MY.SC: myelinating Schwann cells; Mac/Mo: macrophage/monocyte. (D–F) scRNA-seq data from Zhao et al. (2022) [\[3\]](#) (accession number: GSE198582) were merged into a single Seurat object and visualized on UMAP plots. Cell types annotated by Zhao et al. (2022) [\[3\]](#) are shown in (D), and expression levels of (E) *Ret* and (F) *Gfra1* are displayed. cDC: conventional dendritic cells; DCx: dendritic cells destined for homing; dMES: differentiating mesenchymal cells; EC: endothelial cells; eMES: endoneurial mesenchymal cells; Fb: fibroblasts; GC: granulocytes; Mac: macrophages; Mast: mast cells; Mo: monocytes; MoDC: monocyte-derived dendritic cells; NK: natural killer cells; pDC: plasmacytoid dendritic cells; pMES: perineurial mesenchymal cells; prol.MES: proliferating mesenchymal cells; SC: Schwann cells; TC: T cells; vSMC_PC: vascular smooth muscle cells/pericytes; NA: not applicable.



Supplemental figure 2.

Expression of nerve injury-induced, cluster-specific genes in FAPs.

(A–B) Expressions of (A) *Rspo1* and (B) *Csmc1* shown on UMAP plots, separated by samples. scRNA-seq data obtained in this study were used.



Supplemental figure 3.

Expression of *Bdnf* in muscle-resident mononuclear cells affected by denervation.

(A) UMAP plot showing data from Nicoletti et al. (2023) [\[1\]](#) labeled by cell types identified. (B) Expression pattern of *Bdnf* in data from Nicoletti et al. (2023) [\[1\]](#) shown on UMAP plots, separately by days post denervation. (C) Expression of *Bdnf* in each cell type on different days post denervation displayed in violin plots. *P* values were calculated by comparing each injury-affected cells' expression levels versus its uninjured state (0 dpi). Only significant *p* values are shown. Wilcoxon rank sum test.

Key TF	Adjusted P value	List of overlapped genes
Jun	0.000114	Timp1, C1qtnf3, Plaur, Slc39a14, Mmp3, Itga5, Serpine1, Tgfb1, Mmp19, Ccl2, Slc8a1, Plau
Smad3	0.000399	Serpine1, Plau, Nedd9, Acta2, Ccl2, Tagln, Enpp1
Msx2	0.00464	Lss, Enpp1, Tagln, Alpl
Smad1	0.00579	Runx1, Col4a1, Col4a2, Tnfrsf11b
Ppard	0.00579	Angptl4, Tgfb1, Insig1
Sp1	0.00579	Acta2, Trf, Serpine1, Plaur, Lgals1, Mgp, Ccl2, Nes, Adcyap1r1, Itga5, Bmp4, Notch1, Skil
Fos	0.0149	Tgfb1, Bdnf, Tslp, Plau, Pdpn
Tgfb1i1	0.0149	Ccl2, Tgfb1
Srf	0.0185	Tagln, Barx2, Acta2
Id3	0.0298	Notch1, Alpl
Nfkb1	0.0298	Mmp3, Tgfb1, Dmp1, Pla2g4a, Il15, Egr2, Plaur, Ppp1r13l, Ccl2
Junb	0.034	Plau, Serpine1
Pparg	0.034	Serpine1, Muc1, Angptl4, C1qtnf3
Nfkb2	0.0362	Hif1a, Dmp1
Id1	0.0382	Thbs1, Alpl
Runx2	0.0382	Alpl, Mgp, Thbs1, Enpp1
Arntl	0.0382	Cxcl5, Bhlhe41
Msx1	0.0382	Tagln, Bmp4
Nr4a2	0.0382	Tnc, Gch1
Ets1	0.0388	Timp1, Mmp3, Ccl2, Bmp4
Prox1	0.0465	Pdpn, Notch1
Bcl3	0.0465	Runx1, Tnfrsf12a
Clock	0.0465	Serpine1, Bhlhe41
Etv4	0.0465	Mmp3, Plau

Supplemental table 1.

Results from TRRUST showing transcription factors predicted to regulate genes specifically enriched in cluster 2.

Genes known to be regulated by each transcription factor is listed.

Key TF	Adjusted P value	List of overlapped genes
Nfkb1	1.64E-05	Cxcl10, Tnfsf13b, Cebpa, Apoe, Cxcl1, Il12a, Myc, Vcam1, Tnf, Sox9, Plin2, Rel, Igfbp2, Birc3, Hmox1, Nfkbiz, Bcl2
Cebpb	0.000206	Bcl2, Myc, Mafb, Cebpa, Btg2, Serpine1, Socs3
Sp1	0.000206	Ces1d, Myc, Mgarp, Serpine1, Sirt1, Cebpd, Egr1, Apoe, Cebpa, Slc2a3, Socs3, Adcyap1r1, Tnf, Ar, Lpl, Bmp4, Igfbp3
Dlx5	0.000206	Wnt5a, Alpl, Myc, Igfbp3
Stat3	0.000206	Mt1, Il12a, Pnp, Socs3, Bcl2, Cebpd, Egr1, Tnf, Myc
Rela	0.000206	Tnfsf13b, Myc, Vcam1, Igfbp2, Birc3, Pgf, Sox9, Cxcl10, Apoe, Tnf, Bcl2
Stat1	0.000336	Cxcl9, Egr1, Mt1, Socs3, Cebpd, Cxcl10
Id1	0.000336	Thbs1, Alpl, Rel, Tnf
Crebbp	0.000876	Socs3, Fosb, Tnf, Hmox1, Bcl2, Mt1
Rel	0.00115	Cebpd, Birc3, Il12a, Tnf, Myc
Jun	0.00119	Plin2, Cebpd, Cxcl1, Serpine1, Hmox1, Aldh1a1, Tnf, Sirt1, Socs3, Plau
Hnf1b	0.00135	Mafb, Pde4c, Socs3
Hif1a	0.00324	Mt1, Cited2, Hmox1, Serpine1
Tfap2a	0.00381	Apoe, Cebpa, Meis1
Trp53	0.00595	Btg2, Thbs1, Hmox1, Bcl2, Mt1, Agtr1a, Myc, Serpine1, Egr1, Pappa
Ikbkb	0.00595	Cxcl9, Cxcl10, Tnf
Epas1	0.00678	Serpine1, Cited2, Vcam1
Ppara	0.00678	Cebpa, Lpl, Cebpd, Serpine1, Bcl2
Twist1	0.00781	Fgf10, Sox9, Tnf, Mme
Smad3	0.00809	Serpine1, Plau, Sirt1, Tnfsf13b, Myc
Bcl3	0.00899	Tnf, Cxcl10, Ubc
Atf2	0.0104	Sox9, Cebpa, Tnf
Fos	0.0127	Socs3, Tslp, Mt1, Plau, Egr1
Etv2	0.0146	Sox9, Plau
Mtf1	0.0146	Pgf, Mt1
Rbl1	0.0146	Myc, Alpl
Ctnnb1	0.0167	Bmp4, Isl1, Myc, Tbx3, Gja1
Elk1	0.0181	Hmox1, Egr1
Fosl1	0.0181	Thbs1, Thbs2
Dnmt3a	0.0209	Vtn, Mt1
Foxg1	0.0209	Ebf3, Serpine1
Id3	0.0209	Vcam1, Alpl
Tbx1	0.0209	Riply3, Fgf10
Egr1	0.0225	Tnf, Serpine1, Thbs1, Nr4a1, Il12a
Irf1	0.0225	Cxcl10, Il12a, Tnf
Foxo3	0.0225	Socs3, Sirt1
Gfi1b	0.0225	Meis1, Socs3
Junb	0.0225	Plau, Serpine1
Ncoa3	0.0225	Igfbp3, Tbx3
Foxo1	0.0242	Bcl2l11, Egr1, Lpl, Alpl

Supplemental table 2.

Results from TRRUST showing transcription factors predicted to regulate genes specifically enriched in cluster 3.

Genes known to be regulated by each transcription factor is listed.

Myc	0.0242	Myc, Cebpd, Bcl2, Zfp36
Pparg	0.0246	Serpine1, Plin2, Egr1, Hmox1
Nfkb2	0.0246	Myc, Rel
Nr4a1	0.0246	Serpine1, Ar
Nfe2l2	0.0278	Bcl2, Hmox1, Sult1e1, Mt1
Id2	0.0278	Alpl, Zbtb16
Klf5	0.0278	Egr1, Serpine1
Creb1	0.0312	Bcl2, Nfkbiz, Slc2a3
Runx2	0.0336	Alpl, Thbs1, Hbegf, Sox9
Ets1	0.0369	Egr1, Hmox1, Nr2f1, Bmp4
Ep300	0.0382	Tnfsf13b, Mt1, Hmox1, Socs3
Usf2	0.04	Hmox1, Mt1
Mecp2	0.0496	Slc2a3, Igfbp3
Stat6	0.0496	Tnf, Egr1

Supplemental table 2. (continued)

Gene	Secreted	GO term related to neuron/glia cell regulation	Exclusive expression in activated FAPs
<i>Bdnf</i>	O	O	O
<i>Apoe</i>	O	O	X
<i>Ccl2</i>	O	O	X
<i>Tgfb1</i>	O	O	X
<i>Tnf</i>	O	O	X
<i>Vcam1</i>	O	O	X
<i>Dmp1</i>	O	X	O
<i>C1qtnf3</i>	O	X	X
<i>Cxcl1</i>	O	X	X
<i>Cxcl10</i>	O	X	X
<i>Il12a</i>	O	X	X
<i>Il15</i>	O	X	X
<i>Mmp19</i>	O	X	X
<i>Mmp3</i>	O	X	X
<i>Plau</i>	O	X	X
<i>Plaur</i>	O	X	X
<i>Serpine1</i>	O	X	X
<i>Timp1</i>	O	X	X
<i>Tnfsf13b</i>	O	X	X
<i>Tslp</i>	O	X	X
<i>Bcl2</i>	X	O	X
<i>Egr1</i>	X	O	X
<i>Egr2</i>	X	O	X
<i>Hif1a</i>	X	O	X
<i>Hmox1</i>	X	O	X
<i>Igf2bp2</i>	X	O	X
<i>Mt1</i>	X	O	X
<i>Myc</i>	X	O	X
<i>Rel</i>	X	O	X
<i>Sirt1</i>	X	O	X
<i>Sox9</i>	X	O	X
<i>Aldh1a1</i>	X	X	X
<i>Birc3</i>	X	X	X
<i>Cebpa</i>	X	X	X
<i>Cebpd</i>	X	X	X
<i>Itga5</i>	X	X	X
<i>Nfkbiz</i>	X	X	X
<i>Pdpn</i>	X	X	X
<i>Pla2g4a</i>	X	X	X
<i>Plin2</i>	X	X	X
<i>Ppp1r13l</i>	X	X	X
<i>Slc39a14</i>	X	X	X
<i>Slc8a1</i>	X	X	X
<i>Socs3</i>	X	X	X

Supplemental table 3.

Categorization of genes predicted to be regulated by transcription factors that act downstream of the GDNF signaling pathway.

Note that only *Bdnf* fits into all three criteria.

No.	Primer	Usage	Sequence (5' to 3')
1	Prrx1Cre_com_R (P1)	Genotyping PCR	TAG TGA AGT GGA AGT TCC TGG
2	Prrx1Cre_WT_F (P2)	Genotyping PCR	CAG TTC CTA CCC TGA TTT CC
3	Prrx1Cre_Tg_F (P3)	Genotyping PCR	GAT CAT AAT CAG CCA TAC CAC
4	Bdnf_flox_F (P4)	Genotyping PCR	TGT GAT TGT GTT TCT GGT GAC
5	Bdnf_flox_R (P5)	Genotyping PCR	CGG TTT CTA AGC AAG TGA ACA
6	Bdnf_recomb_R (P6)	Genotyping PCR	GAA ATT TTC TCC ATC CCT ACT CCG GG
7	Cre_F	Genotyping PCR	GCA TTA CCG GTC GAT GCA ACG AGT GAT GAG
8	Cre_R	Genotyping PCR	GAG TGA ACG AAC CTG GTC GAA ATC AGT GCG
9	Rosa-tdT_WT_F	Genotyping PCR	AAG GGA GCT GCA GTG GAG TA
10	Rosa-tdT_WT_R	Genotyping PCR	CCG AAA ATC TGT GGG AAG TC
11	Rosa-tdT_Tg_F	Genotyping PCR	GGC ATT AAA GCA GCG TAT CC
12	Rosa-tdT_Tg_R	Genotyping PCR	CTG TTC CTG TAC GGC ATG G
13	Actb_qF	RT-qPCR	CCT CCC TGG AGA AGA GCT ATG
14	Actb_qR	RT-qPCR	TTA CGG ATG TCA ACG TCA CAC
15	Ret_qF	RT-qPCR	CCA GGG CTT CCC AAT CAG TT
16	Ret_qR	RT-qPCR	TTC CAA ACT CGC CTT CTC CC
17	Gfra1_qF	RT-qPCR	CAC TCC TGG ATT TGC TGA TGT
18	Gfra1_qR	RT-qPCR	AGT GTG CGG TAC TTG GTG C
19	Gdnf_qF	RT-qPCR	TCG GCC GAG ACA ATG TAT GA
20	Gdnf_qR	RT-qPCR	CAA CAT GCC TGG CCT ACT TTG
21	Bdnf_qF	RT-qPCR	AAG GAC GCG GAC TTG TAC AC
22	Bdnf_qR	RT-qPCR	CGC TAA TAC TGT CAC ACA CGC

Supplemental table 4.

Primers used in this study for genotyping PCR or RT-qPCR.

References

- Airaksinen MS, Saarma M (2002) **The GDNF family: signalling, biological functions and therapeutic value** *Nat Rev Neurosci* **3**:383–94 <https://doi.org/10.1038/nrn812>
- Arthur-Farraj PJ *et al.* (2012) **c-Jun reprograms Schwann cells of injured nerves to generate a repair cell essential for regeneration** *Neuron* **75**:633–47 <https://doi.org/10.1016/j.neuron.2012.06.021>
- Aurora AB, Olson EN (2014) **Immune modulation of stem cells and regeneration** *Cell Stem Cell* **15**:14–25 <https://doi.org/10.1016/j.stem.2014.06.009>
- Bakooshli MA, Wang YX, Monti E, Su S, Kraft P, Nalbandian M, Alexandrova L, Wheeler JR, Vogel H, Blau HM (2023) **Regeneration of neuromuscular synapses after acute and chronic denervation by inhibiting the gerozyme 15-prostaglandin dehydrogenase** *Science Translational Medicine* **15** <https://doi.org/10.1126/scitranslmed.adg1485>
- Baydyuk M, Xu B (2014) **BDNF signaling and survival of striatal neurons** *Front Cell Neurosci* **8** <https://doi.org/10.3389/fncel.2014.00254>
- Buttner R, Schulz A, Reuter M, Akula AK, Mindos T, Carlstedt A, Riecken LB, Baader SL, Bauer R, Morrison H (2018) **Inflammaging impairs peripheral nerve maintenance and regeneration** *Aging Cell* **17** <https://doi.org/10.1111/accel.12833>
- Carr MJ, Toma JS, Johnston APW, Steadman PE, Yuzwa SA, Mahmud N, Frankland PW, Kaplan DR, Miller FD (2019) **Mesenchymal Precursor Cells in Adult Nerves Contribute to Mammalian Tissue Repair and Regeneration** *Cell Stem Cell* **24**:240–256 <https://doi.org/10.1016/j.stem.2018.10.024>
- Chan JR, Cosgaya JM, Wu YJ, Shooter EM (2001) **Neurotrophins are key mediators of the myelination program in the peripheral nervous system** *Proceedings of the National Academy of Sciences* **98**:14661–14668
- Chung T, Prasad K, Lloyd TE (2014) **Peripheral neuropathy: clinical and electrophysiological considerations** *Neuroimaging Clin N Am* **24**:49–65 <https://doi.org/10.1016/j.nic.2013.03.023>
- Cintron-Colon AF, Almeida-Alves G, Boynton AM, Spitsbergen JM (2020) **GDNF synthesis, signaling, and retrograde transport in motor neurons** *Cell Tissue Res* **382**:47–56 <https://doi.org/10.1007/s00441-020-03287-6>
- Contreras O, Rebolledo DL, Oyarzun JE, Olguin HC, Brandan E (2016) **Connective tissue cells expressing fibro/adipogenic progenitor markers increase under chronic damage: relevance in fibroblast-myofibroblast differentiation and skeletal muscle fibrosis** *Cell Tissue Res* **364**:647–660 <https://doi.org/10.1007/s00441-015-2343-0>
- Contreras O, Rossi FMV, Theret M (2021) **Origins, potency, and heterogeneity of skeletal muscle fibro-adipogenic progenitors-time for new definitions** *Skelet Muscle* **11** <https://doi.org/10.1186/s13395-021-00265-6>

- De Micheli AJ, Laurillard EJ, Heinke CL, Ravichandran H, Fraczek P, Soueid-Baumgarten S, De Vlaminck I, Elemento O, Cosgrove BD (2020) **Single-Cell Analysis of the Muscle Stem Cell Hierarchy Identifies Heterotypic Communication Signals Involved in Skeletal Muscle Regeneration** *Cell Rep* **30**:3583–3595 <https://doi.org/10.1016/j.celrep.2020.02.067>
- Doerflinger NH, Macklin WB, Popko B (2003) **Inducible site-specific recombination in myelinating cells** *Genesis* **35**:63–72 <https://doi.org/10.1002/gene.10154>
- Encinas M, Tansey MG, Tsui-Pierchala BA, Comella JX, Milbrandt J, Johnson EM (2001) **c-Src is required for glial cell line-derived neurotrophic factor (GDNF) family ligand-mediated neuronal survival via a phosphatidylinositol-3 kinase (PI-3K)-dependent pathway** *Journal of Neuroscience* **21**:1464–1472
- English AW, Liu K, Nicolini JM, Mulligan AM, Ye K (2013) **Small-molecule trkB agonists promote axon regeneration in cut peripheral nerves** *Proc Natl Acad Sci U S A* **110**:16217–22 <https://doi.org/10.1073/pnas.1303646110>
- Fielder GC, Yang TW, Razdan M, Li Y, Lu J, Perry JK, Lobie PE, Liu DX (2018) **The GDNF Family: A Role in Cancer?** *Neoplasia* **20**:99–117 <https://doi.org/10.1016/j.neo.2017.10.010>
- Forese MG, Pellegatta M, Canevazzi P, Gullotta GS, Podini P, Rivellini C, Previtali SC, Bacigaluppi M, Quattrini A, Taveggia C (2020) **Prostaglandin D2 synthase modulates macrophage activity and accumulation in injured peripheral nerves** *Glia* **68**:95–110 <https://doi.org/10.1002/glia.23705>
- Ghosh A, Carnahan J, Greenberg ME (1994) **Requirement for BDNF in activity-dependent survival of cortical neurons** *Science* **263**:1618–1623 <https://doi.org/10.1126/science.7907431>
- Goebbels S *et al.* (2010) **Elevated phosphatidylinositol 3,4,5-trisphosphate in glia triggers cell-autonomous membrane wrapping and myelination** *J Neurosci* **30**:8953–64 <https://doi.org/10.1523/JNEUROSCI.0219-10.2010>
- Gonzalez D, Contreras O, Rebolledo DL, Espinoza JP, van Zundert B, Brandan E (2017) **ALS skeletal muscle shows enhanced TGF-beta signaling, fibrosis and induction of fibro/adipogenic progenitor markers** *PLoS One* **12** <https://doi.org/10.1371/journal.pone.0177649>
- Grinsell D, Keating CP (2014) **Peripheral nerve reconstruction after injury: a review of clinical and experimental therapies** *Biomed Res Int* **2014** <https://doi.org/10.1155/2014/698256>
- Hammarberg H, Piehl F, Cullheim S, Fjell J, Hokfelt T, Fried K (1996) **GDNF mRNA in Schwann cells and DRG satellite cells after chronic sciatic nerve injury** *NeuroReport* **7**:857–860 <https://doi.org/10.1097/00001756-199603220-00004>
- Han H *et al.* (2018) **TRRUST v2: an expanded reference database of human and mouse transcriptional regulatory interactions** *Nucleic Acids Res* **46**:D380–D386 <https://doi.org/10.1093/nar/gkx1013>
- Hann SH, Kim SY, Kim YL, Jo YW, Kang JS, Park H, Choi SY, Kong YY (2024) **Depletion of SMN protein in mesenchymal progenitors impairs the development of bone and neuromuscular junction in spinal muscular atrophy** *Elife* **12**

Hanz S *et al.* (2003) **Axoplasmic importins enable retrograde injury signaling in lesioned nerve** *Neuron* **40**:1095–1104 [https://doi.org/10.1016/s0896-6273\(03\)00770-0](https://doi.org/10.1016/s0896-6273(03)00770-0)

Hao Y *et al.* (2021) **Integrated analysis of multimodal single-cell data** *Cell* **184**:3573–3587 <https://doi.org/10.1016/j.cell.2021.04.048>

Heredia JE, Mukundan L, Chen FM, Mueller AA, Deo RC, Locksley RM, Rando TA, Chawla A (2013) **Type 2 innate signals stimulate fibro/adipogenic progenitors to facilitate muscle regeneration** *Cell* **153**:376–88 <https://doi.org/10.1016/j.cell.2013.02.053>

Hoke A, Gordon T, Zochodne DW, Sulaiman OA (2002) **A decline in glial cell-line-derived neurotrophic factor expression is associated with impaired regeneration after long-term Schwann cell denervation** *Exp Neurol* **173**:77–85 <https://doi.org/10.1006/exnr.2001.7826>

Jing S, Wen D, Yu Y, Holst PL, Luo Y, Fang M, Tamir R, Antonio L, Hu Z, Cupples R (1996) **GDNF-induced activation of the ret protein tyrosine kinase is mediated by GDNFR- α , a novel receptor for GDNF** *Cell* **85**:1113–1124

Joe AW, Yi L, Natarajan A, Le Grand F, So L, Wang J, Rudnicki MA, Rossi FM (2010) **Muscle injury activates resident fibro/adipogenic progenitors that facilitate myogenesis** *Nat Cell Biol* **12**:153–63 <https://doi.org/10.1038/ncb2015>

Joe AW, Yi L, Natarajan A, Le Grand F, So L, Wang J, Rudnicki MA, Rossi FM (2010) **Muscle injury activates resident fibro/adipogenic progenitors that facilitate myogenesis** *Nature cell biology* **12**:153–163

Joseph NM, Mukoyama YS, Mosher JT, Jaegle M, Crone SA, Dormand EL, Lee KF, Meijer D, Anderson DJ, Morrison SJ (2004) **Neural crest stem cells undergo multilineage differentiation in developing peripheral nerves to generate endoneurial fibroblasts in addition to Schwann cells** *Development* **131**:5599–612 <https://doi.org/10.1242/dev.01429>

Julier Z, Park AJ, Briquez PS, Martino MM (2017) **Promoting tissue regeneration by modulating the immune system** *Acta Biomater* **53**:13–28 <https://doi.org/10.1016/j.actbio.2017.01.056>

Kalinski AL *et al.* (2020) **Analysis of the immune response to sciatic nerve injury identifies efferocytosis as a key mechanism of nerve debridement** *Elife* **9** <https://doi.org/10.7554/eLife.60223>

Kanehisa M, Furumichi M, Sato Y, Kawashima M, Ishiguro-Watanabe M (2023) **KEGG for taxonomy-based analysis of pathways and genomes** *Nucleic Acids Res* **51**:D587–D592 <https://doi.org/10.1093/nar/gkac963>

Kim JH *et al.* (2022) **Bap1/SMN axis in Dpp4+ skeletal muscle mesenchymal cells regulates the neuromuscular system** *JCI Insight* **7** <https://doi.org/10.1172/jci.insight.158380>

Kolberg L, Raudvere U, Kuzmin I, Adler P, Vilo J, Peterson H (2023) **g:Profiler-interoperable web service for functional enrichment analysis and gene identifier mapping (2023 update)** *Nucleic Acids Res* **51**:W207–W212 <https://doi.org/10.1093/nar/gkad347>

Kucera M, Isserlin R, Arkhangorodsky A, Bader GD (2016) **AutoAnnotate: A Cytoscape app for summarizing networks with semantic annotations** *F1000Res* **5** <https://doi.org/10.12688/f1000research.9090.1>

La Manno G *et al.* (2018) **RNA velocity of single cells** *Nature* **560**:494–498 <https://doi.org/10.1038/s41586-018-0414-6>

Leinroth AP, Mirando AJ, Rouse D, Kobayahsi Y, Tata PR, Rueckert HE, Liao Y, Long JT, Chakkalakal JV, Hilton MJ (2022) **Identification of distinct non-myogenic skeletal-muscle-resident mesenchymal cell populations** *Cell Rep* **39** <https://doi.org/10.1016/j.celrep.2022.110785>

Lemos DR, Babaeijandaghi F, Low M, Chang CK, Lee ST, Fiore D, Zhang RH, Natarajan A, Nedospasov SA, Rossi FM (2015) **Nilotinib reduces muscle fibrosis in chronic muscle injury by promoting TNF-mediated apoptosis of fibro/adipogenic progenitors** *Nat Med* **21**:786–94 <https://doi.org/10.1038/nm.3869>

Lieberman B, Kusi M, Hung CN, Chou CW, He N, Ho YY, Taverna JA, Huang THM, Chen CL (2021) **Toward uncharted territory of cellular heterogeneity: advances and applications of single-cell RNA-seq** *J Transl Genet Genom* **5**:1–21 <https://doi.org/10.20517/jtgg.2020.51>

Lin H, Ma X, Sun Y, Peng H, Wang Y, Thomas SS, Hu Z (2022) **Decoding the transcriptome of denervated muscle at single-nucleus resolution** *J Cachexia Sarcopenia Muscle* **13**:2102–2117 <https://doi.org/10.1002/jcsm.13023>

Liu L, Cheung TH, Charville GW, Rando TA (2015) **Isolation of skeletal muscle stem cells by fluorescence-activated cell sorting** *Nat Protoc* **10**:1612–24 <https://doi.org/10.1038/nprot.2015.110>

Logan M, Martin JF, Nagy A, Lobe C, Olson EN, Tabin CJ (2002) **Expression of Cre Recombinase in the developing mouse limb bud driven by a Prxl enhancer** *Genesis* **33**:77–80 <https://doi.org/10.1002/gene.10092>

Lukjanenko L *et al.* (2019) **Aging Disrupts Muscle Stem Cell Function by Impairing Matricellular WISP1 Secretion from Fibro-Adipogenic Progenitors** *Cell Stem Cell* **24**:433–446 <https://doi.org/10.1016/j.stem.2018.12.014>

Madaro L *et al.* (2018) **Denervation-activated STAT3-IL-6 signalling in fibro-adipogenic progenitors promotes myofibres atrophy and fibrosis** *Nat Cell Biol* **20**:917–927 <https://doi.org/10.1038/s41556-018-0151-y>

Magill CK, Tong A, Kawamura D, Hayashi A, Hunter DA, Parsadanian A, Mackinnon SE, Myckatyn TM (2007) **Reinnervation of the tibialis anterior following sciatic nerve crush injury: a confocal microscopic study in transgenic mice** *Exp Neurol* **207**:64–74 <https://doi.org/10.1016/j.expneurol.2007.05.028>

Maita KC, Garcia JP, Avila FR, Torres-Guzman RA, Ho O, Chini CCS, Chini EN, Forte AJ (2023) **Evaluation of the Aging Effect on Peripheral Nerve Regeneration: A Systematic Review** *J Surg Res* **288**:329–340 <https://doi.org/10.1016/j.jss.2023.03.017>

Malecova B *et al.* (2018) **Dynamics of cellular states of fibro-adipogenic progenitors during myogenesis and muscular dystrophy** *Nat Commun* **9** <https://doi.org/10.1038/s41467-018-06068-6>

Mallik A, Weir AI (2005) **Nerve conduction studies: essentials and pitfalls in practice** *J Neurol Neurosurg Psychiatry* **76** <https://doi.org/10.1136/jnnp.2005.069138>

- Merico D, Isserlin R, Stueker O, Emili A, Bader GD (2010) **Enrichment map: a network-based method for gene-set enrichment visualization and interpretation** *PLoS One* **5** <https://doi.org/10.1371/journal.pone.0013984>
- Mueller M, Wacker K, Ringelstein EB, Hickey WF, Imai Y, Kiefer R (2001) **Rapid response of identified resident endoneurial macrophages to nerve injury** *Am J Pathol* **159**:2187–97 [https://doi.org/10.1016/S0002-9440\(10\)63070-2](https://doi.org/10.1016/S0002-9440(10)63070-2)
- Murphy MM, Lawson JA, Mathew SJ, Hutcheson DA, Kardon G (2011) **Satellite cells, connective tissue fibroblasts and their interactions are crucial for muscle regeneration** *Development* **138**:3625–37 <https://doi.org/10.1242/dev.064162>
- Nicoletti C, Wei X, Etxaniz U, D’Ercole C, Madaro L, Perera R, Puri PL (2023) **Muscle denervation promotes functional interactions between glial and mesenchymal cells through NGFR and NGF** *iScience* **26** <https://doi.org/10.1016/j.isci.2023.107114>
- Nicoletti C, Wei X, Etxaniz U, Proietti D, Madaro L, Puri PL (2020) **scRNA-seq-based analysis of skeletal muscle response to denervation reveals selective activation of muscle-resident glial cells and fibroblasts** *Biorxiv* <https://doi.org/10.1101/2020.12.29.424762>
- Oprescu SN, Yue F, Qiu J, Brito LF, Kuang S (2020) **Temporal Dynamics and Heterogeneity of Cell Populations during Skeletal Muscle Regeneration** *iScience* **23** <https://doi.org/10.1016/j.isci.2020.100993>
- Ortega-Gomez A, Perretti M, Soehnlein O (2013) **Resolution of inflammation: an integrated view** *EMBO Mol Med* **5**:661–74 <https://doi.org/10.1002/emmm.201202382>
- Oudega M, Hagg T (1999) **Neurotrophins promote regeneration of sensory axons in the adult rat spinal cord** *Brain Research* **818**:431–438
- Painter MW *et al.* (2014) **Diminished Schwann cell repair responses underlie age-associated impaired axonal regeneration** *Neuron* **83**:331–343 <https://doi.org/10.1016/j.neuron.2014.06.016>
- Parrinello S, Napoli I, Ribeiro S, Wingfield Digby P, Fedorova M, Parkinson DB, Doddrell RD, Nakayama M, Adams RH, Lloyd AC (2010) **EphB signaling directs peripheral nerve regeneration through Sox2-dependent Schwann cell sorting** *Cell* **143**:145–55 <https://doi.org/10.1016/j.cell.2010.08.039>
- Proietti D *et al.* (2021) **Activation of skeletal muscle-resident glial cells upon nerve injury** *JCI Insight* **6** <https://doi.org/10.1172/jci.insight.143469>
- Reimand J *et al.* (2019) **Pathway enrichment analysis and visualization of omics data using g:Profiler, GSEA, Cytoscape and EnrichmentMap** *Nat Protoc* **14**:482–517 <https://doi.org/10.1038/s41596-018-0103-9>
- Roberts EW *et al.* (2013) **Depletion of stromal cells expressing fibroblast activation protein-alpha from skeletal muscle and bone marrow results in cachexia and anemia** *J Exp Med* **210**:1137–51 <https://doi.org/10.1084/jem.20122344>
- Saito Y, Chikenji TS, Matsumura T, Nakano M, Fujimiya M (2020) **Exercise enhances skeletal muscle regeneration by promoting senescence in fibro-adipogenic progenitors** *Nat Commun* **11** <https://doi.org/10.1038/s41467-020-14734-x>

- Sariola H, Saarma M (2003) **Novel functions and signalling pathways for GDNF** *J Cell Sci* **116**:3855–62 <https://doi.org/10.1242/jcs.00786>
- Scheib J, Hoke A (2013) **Advances in peripheral nerve regeneration** *Nat Rev Neurol* **9**:668–76 <https://doi.org/10.1038/nrneurol.2013.227>
- Scheib JL, Hoke A (2016) **An attenuated immune response by Schwann cells and macrophages inhibits nerve regeneration in aged rats** *Neurobiol Aging* **45**:1–9 <https://doi.org/10.1016/j.neurobiolaging.2016.05.004>
- Scott RW, Arostegui M, Schweitzer R, Rossi FMV, Underhill TM (2019) **Hic1 Defines Quiescent Mesenchymal Progenitor Subpopulations with Distinct Functions and Fates in Skeletal Muscle Regeneration** *Cell Stem Cell* **25**:797–813 <https://doi.org/10.1016/j.stem.2019.11.004>
- Shannon P, Markiel A, Ozier O, Baliga NS, Wang JT, Ramage D, Amin N, Schwikowski B, Ideker T (2003) **Cytoscape: a software environment for integrated models of biomolecular interaction networks** *Genome Res* **13**:2498–504 <https://doi.org/10.1101/gr.1239303>
- Takemura Y *et al.* (2012) **Brain-derived neurotrophic factor from bone marrow-derived cells promotes post-injury repair of peripheral nerve** *PLoS One* **7** <https://doi.org/10.1371/journal.pone.0044592>
- Theret M, Rossi FMV, Contreras O (2021) **Evolving Roles of Muscle-Resident Fibro-Adipogenic Progenitors in Health, Regeneration, Neuromuscular Disorders, and Aging** *Front Physiol* **12** <https://doi.org/10.3389/fphys.2021.673404>
- Toma JS, Karamboulas K, Carr MJ, Kolaj A, Yuzwa SA, Mahmud N, Storer MA, Kaplan DR, Miller FD (2020) **Peripheral Nerve Single-Cell Analysis Identifies Mesenchymal Ligands that Promote Axonal Growth** *eNeuro* **7** <https://doi.org/10.1523/ENEURO.0066-20.2020>
- Treanor JJ, Goodman L, de Sauvage F, Stone DM, Poulsen KT, Beck CD, Gray C, Armanini MP, Pollock RA, Hefti F (1996) **Characterization of a multicomponent receptor for GDNF** *Nature* **382**:80–83
- Trupp M *et al.* (1996) **Functional receptor for GDNF encoded by the c-ret proto-oncogene** *Nature* **381**:785–789 <https://doi.org/10.1038/381785a0>
- Uezumi A, Fukada S-i, Yamamoto N, Si Takeda, Tsuchida K (2010) **Mesenchymal progenitors distinct from satellite cells contribute to ectopic fat cell formation in skeletal muscle** *Nature cell biology* **12**:143–152
- Uezumi A, Fukada S, Yamamoto N, Takeda S, Tsuchida K (2010) **Mesenchymal progenitors distinct from satellite cells contribute to ectopic fat cell formation in skeletal muscle** *Nat Cell Biol* **12**:143–52 <https://doi.org/10.1038/ncb2014>
- Uezumi A, Ikemoto-Uezumi M, Tsuchida K (2014) **Roles of nonmyogenic mesenchymal progenitors in pathogenesis and regeneration of skeletal muscle** *Front Physiol* **5** <https://doi.org/10.3389/fphys.2014.00068>
- Uezumi A *et al.* (2021) **Mesenchymal Bmp3b expression maintains skeletal muscle integrity and decreases in age-related sarcopenia** *J Clin Invest* **131** <https://doi.org/10.1172/JCI139617>
- Uezumi A *et al.* (2011) **Fibrosis and adipogenesis originate from a common mesenchymal progenitor in skeletal muscle** *J Cell Sci* **124**:3654–64 <https://doi.org/10.1242/jcs.086629>

Vallecillo-Garcia P *et al.* (2017) **Odd skipped-related 1 identifies a population of embryonic fibro-adipogenic progenitors regulating myogenesis during limb development** *Nat Commun* **8** <https://doi.org/10.1038/s41467-017-01120-3>

Verdú E, Ceballos D, Vilches JJ, Navarro X (2008) **Influence of aging on peripheral nerve function and regeneration** *Journal of the Peripheral Nervous System* **5**:191–208 <https://doi.org/10.1111/j.1529-8027.2000.00026.x>

Wagstaff LJ *et al.* (2021) **Failures of nerve regeneration caused by aging or chronic denervation are rescued by restoring Schwann cell c-Jun** *Elife* **10** <https://doi.org/10.7554/eLife.62232>

Wilhelm JC, Xu M, Cucoranu D, Chmielewski S, Holmes T, Lau KS, Bassell GJ, English AW (2012) **Cooperative roles of BDNF expression in neurons and Schwann cells are modulated by exercise to facilitate nerve regeneration** *J Neurosci* **32**:5002–9 <https://doi.org/10.1523/JNEUROSCI.1411-11.2012>

Wosczyzna MN, Konishi CT, Perez Carbajal EE, Wang TT, Walsh RA, Gan Q, Wagner MW, Rando TA (2019) **Mesenchymal Stromal Cells Are Required for Regeneration and Homeostatic Maintenance of Skeletal Muscle** *Cell Rep* **27**:2029–2035 <https://doi.org/10.1016/j.celrep.2019.04.074>

Xiao J, Wong AW, Willingham MM, Kaasinen SK, Hendry IA, Howitt J, Putz U, Barrett GL, Kilpatrick TJ, Murray SS (2009) **BDNF exerts contrasting effects on peripheral myelination of NGF-dependent and BDNF-dependent DRG neurons** *J Neurosci* **29**:4016–22 <https://doi.org/10.1523/JNEUROSCI.3811-08.2009>

Xu P, Rosen KM, Hedstrom K, Rey O, Guha S, Hart C, Corfas G (2013) **Nerve injury induces glial cell line-derived neurotrophic factor (GDNF) expression in Schwann cells through purinergic signaling and the PKC-PKD pathway** *Glia* **61**:1029–40 <https://doi.org/10.1002/glia.22491>

Zhang JY, Luo XG, Xian CJ, Liu ZH, Zhou XF (2000) **Endogenous BDNF is required for myelination and regeneration of injured sciatic nerve in rodents** *European Journal of Neuroscience* **12**:4171–4180 <https://doi.org/10.1111/j.1460-9568.2000.01312.x>

Zhao XF *et al.* (2022) **The injured sciatic nerve atlas (iSNAT), insights into the cellular and molecular basis of neural tissue degeneration and regeneration** *Elife* **11** <https://doi.org/10.7554/eLife.80881>

Zheng J, Sun J, Lu X, Zhao P, Li K, Li L (2016) **BDNF promotes the axonal regrowth after sciatic nerve crush through intrinsic neuronal capability upregulation and distal portion protection** *Neurosci Lett* **621**:1–8 <https://doi.org/10.1016/j.neulet.2016.04.006>

Editors

Reviewing Editor

Moses Chao

New York University Langone Medical Center, New York, United States of America

Senior Editor

Sacha Nelson

Brandeis University, Waltham, United States of America

Reviewer #1 (Public Review):

In this manuscript, Yoo et al describe the role of a specialized cell type found in muscle, Fibro-adipogenic progenitors (FAPs), in promoting regeneration following sciatic nerve injury. Using single-cell transcriptomics, they characterize the expression profiles of FAPs at various times after nerve crush or denervation. Their results reveal that a population of these muscle-resident mesenchymal progenitors up regulate the receptors for GDNF, which is secreted by Schwann cells following crush injury, suggesting that FAPs respond to this growth factor. They also find that FAPs increase expression of BDNF, which promotes nerve regeneration. The authors demonstrate FAP production of BDNF in vivo is up regulated in response to injection of GDNF and that conditional deletion of BDNF in FAPs results in delayed nerve regeneration after crush injury, primarily due to lagging remyelination. Finally, they also find reduced BDNF expression following crush injury in aged mice, suggesting a potential mechanism to explain the decrease in peripheral nerve regenerative capability in aged animals. These results are very interesting and novel and provide important insights into the mechanisms regulating peripheral nerve regeneration, which has important clinical implications for understanding and treating nerve injuries.

However, the authors should provide more compelling evidence that BDNF is produced by FAPs in response to GDNF signaling. The suggestion that Schwann cell-derived GDNF is responsible for up regulation of BDNF in the FAPs is primarily indirect, based on the data showing that injection of GDNF into the muscle is sufficient to up regulate BDNF (Fig. 4H). The authors more directly test their hypothesis by administering GDNF blocking antibody and find a trend toward reduced BDNF (Fig. 4S2), but it is not statistically significant at this point. Additional replicates should be performed to determine if BDNF levels are indeed reduced when GDNF is blocked.

<https://doi.org/10.7554/eLife.97662.2.sa1>

Author response:

The following is the authors' response to the original reviews.

Point-by-point reply in response to the Reviewer's comments

Reviewer #1

Public review:

[1] (a) Given that only a fraction of the FAPs express BDNF after injury, the authors need to demonstrate the specificity of the Prrx1-Cre for FAPs. This is particularly important because muscle stem cell also express GDNF receptors (Fig. 3C & D) and myogenic progenitors/satellite cells produce BDNF after nerve injury (Griesbeck et al., 1995 (PMID 8531223); Omura et al., 2005 (PMID 16221288)). (b) Moreover, as the authors point out, there are multipotent mesenchymal precursor cells in the nerve that migrate into the surrounding tissue following nerve injury and contribute to regeneration (Carr et al, PMID 30503141). Therefore, there are multiple possible sources of BDNF, highlighting the need to clearly demonstrate that FAP-derived BDNF is essential.

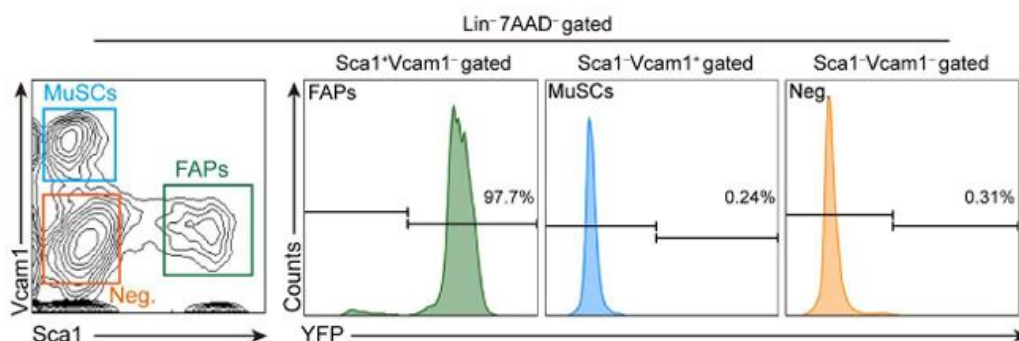
- (a) As the Reviewer noted, both GDNF receptor expression and increased BDNF expression in response to nerve injury are detectable in both FAPs and muscle stem cells (MuSCs).

Therefore, we agree with the Reviewer that demonstrating the specificity of *Prrx1*-Cre in FAPs is crucial to support our claim. In our previous publication (Kim et al., 2022), using *Prrx1*-Cre; Rosa-eYFP mice, we showed that while most of the CD31-CD45-Vcam1-Sca1⁺ FAPs are eYFP⁺, CD31-CD45-Vcam1-Sca1⁻ MuSCs do not express eYFP (Liu et al., 2015; Kim et al., 2022) (Attached Figure 1). Additionally, genomic DNA PCR using mononuclear cells sorted from our *Prrx1*Cre; *Bdnf*^{fl/fl} mice showed that DNA recombination in the floxed *Bdnf* gene could only be detected in FAPs and CD31-CD45-Vcam1-Sca1⁻ cells, but not in MuSCs (Author response image 2). This is consistent with a previous report that showed *Prrx1*-Cre activity in FAPs, pericytes, vascular smooth muscle cells (vSMCs) and tenocytes (Leinroth et al.,

2022), where pericytes, vSMCs and tenocytes are included the CD31-CD45-Vcam1-Sca1⁻ population (Giordani et al., 2019). Together, these results demonstrate that while *Prrx1*-Cre is active in FAPs, it is absent in MuSCs.

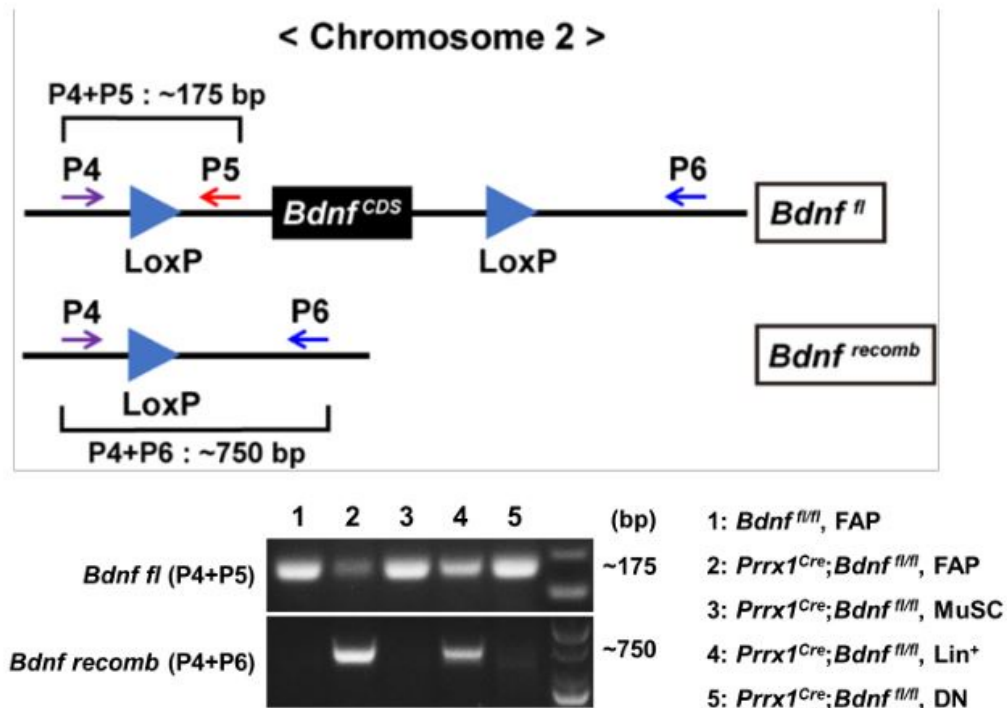
Author response image 1.

Expression of eYFP in muscle-resident, lineage-negative, live mononuclear cells isolated from *Prrx1*Cre;Rosa^{eYFP} mice. Supplemental Figure 3A from Kim et al., 2022. Lin⁻: lineage-negative (CD31-CD45⁻); Neg.: Vcam1-Sca1⁻.



Author response image 2.

Recombination of the floxed *Bdnf* gene in the mononuclear cells sorted from muscles of *Prrx1*Cre; *Bdnf*^{fl/fl} or *Bdnf*^{fl/fl} mice. Genotypes and cell types sampled for each lane is specified. P4, P5, and P6 indicate primers used for each PCR. Lin⁺: lineage(CD31/CD45)-positive; DN: CD31-CD45-Vcam1-Sca1⁻.



(b) We appreciate and agree with the Reviewer's comment that additional experiments are needed to confirm that FAP-derived BDNF is indeed essential for nerve regeneration, considering other potential cellular sources of BDNF, such as nerve-resident mesenchymal precursor cells. One possible experiment that could demonstrate the requirement of FAP-derived BDNF in nerve regeneration would be the transplantation of wild-type FAPs into our *Prrx1*^{Cre}; *Bdnf*^{fl/fl} mice and to see if the delay in nerve regeneration and remyelination is recovered, making the process similar to that in control mice. Unfortunately, since the genetic background of our *Prrx1*^{Cre}; *Bdnf*^{fl/fl} mice is a mixture of B6, 129S4, and BALB/c, immune rejection of the transplanted cells may occur, which makes the experiment technically difficult. Another experimental approach could involve the use of FAP-specific Cre mouse line, as we have mentioned in the Discussion of our original manuscript. However, such a line does not yet exist due to the lack of a marker gene that is expressed specifically in FAPs, but not in nerve-resident mesenchymal precursor cells. Overcoming such technical challenges and demonstrating the requirement of FAP-derived BDNF in nerve regeneration would significantly strengthen our report, though we regret that these methods are currently unavailable.

[2] Similarly, the authors should provide some evidence that BDNF protein is produced by FAPs. All of their data for BDNF expression is based on mRNA expression and that appears to only be increased in a small subset of FAPs. Perhaps an immunostaining could be done to demonstrate up-regulation of BDNF in FAPs after injury.

- We appreciate the Reviewer's constructive comment. To demonstrate that BDNF protein is produced by FAPs upon nerve injury, we performed western blot analysis. FAPs were isolated from either sciatic nerve crush injury-affected muscles at 7 days post injury (dpi) or from the contralateral, uninjured muscles, and protein samples were prepared for SDS-PAGE and western blot using anti-BDNF, anti-PDGFRα and antiGAPDH antibodies. As a result, while both nerve injury-affected and uninjured musclederived FAPs expressed PDGFRα, the mature form of BDNF protein was only detected in nerve injury-affected FAPs, showing that BDNF is indeed expressed in FAPs at the protein level after injury. We have added this new result as

Figure 4F in the New Figure 4 with the experimental scheme as New Figure 4—figure supplement 1, and revised the Results section (lines 364-374) and the Materials and Methods section (lines 687-705) in our manuscript to include the new results in detail.

[3] The suggestion that Schwann cell-derived GDNF is responsible for upregulation of BDNF in the FAPs is indirect, based largely on the data showing that injection of GDNF into the muscle is sufficient to up-regulate BDNF (Fig. 4F & G). However, to more directly connect the 2 observations in a causal way, the authors should inject a Ret/GDNF antagonist, such as a Ret-Fc construct, then measure the BDNF levels.

- We appreciate the Reviewer's constructive comment, and we agree that testing the necessity of GDNF/RET signaling in BDNF upregulation is crucial to link the expression of the two neurotrophic factors in a causal way. As a means to antagonize GDNF/RET signaling, we injected anti-GDNF antibodies into the tibialis anterior and gastrocnemius muscles following sciatic nerve crush injury to block the activity of intramuscular GDNF protein. As a result, although the differences were not statistically significant, we observed a tendency towards decreased *Bdnf* mRNA expression upon anti-GDNF injection compared to IgG controls. We have added this new result as New Figure 4—figure supplement 2, and revised our manuscript to include the details in both the Results section (lines 381-390) and the Materials and Methods section (lines 611-616). We have also changed the title of New Figure 4 (line 332) to encompass the new results. We are aware that further experiments that may involve increasing the number of animals tested, increasing the antibody injection dosage or frequency, or implementation of genetic models such as *Plp1CreER*; *Gdnffl/fl* should be carried out to validate our hypothesis with statistical significance. Unfortunately, due to limited time, resources, and research funds, we were unable to perform such additional experiments. We hope that the Reviewer understands these limitations.

[4] (a) In assessing the regeneration after nerve crush, the authors focus on remyelination, for example, assessing CMAP and g-ratios. However, they should also quantify axon regeneration, which can be done distal to the crush injury at earlier time points, before the 6 weeks scored in their study. Evaluating axon regeneration, which occurs prior to remyelination, would be especially useful because BDNF can act on both Schwann cells, to promote myelination, and axons, enhancing survival and growth. (b) They could also evaluate the stability of the neuromuscular junctions, particularly if a denervation was done with the conditional knock outs, although that may be a bit beyond the scope of this study.

- (a) As the Reviewer mentioned, BDNF is known to act on both Schwann cells and axons, where it promotes myelination and axonal growth, respectively (Oudega and

Hagg, 1998; Zhang et al., 2000; Chan et al., 2001; Xiao et al., 2009; English et al.,

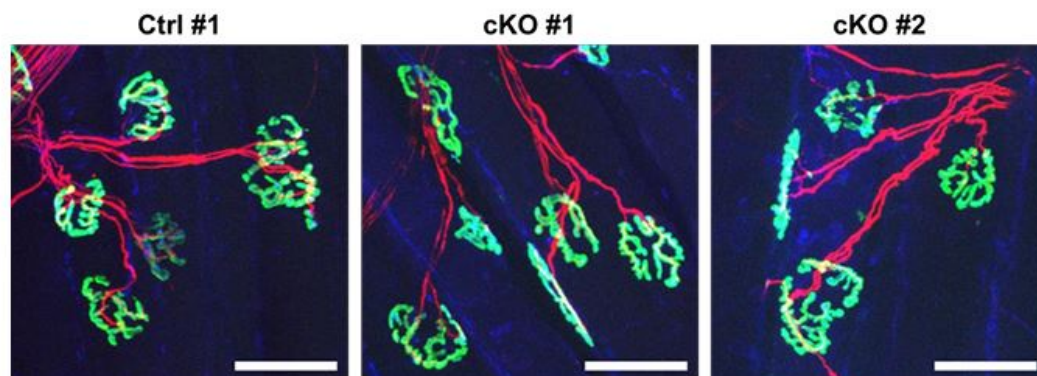
2013). We fully agree with the Reviewer's comment that quantification of axon regeneration, which could be achieved through immunostaining of the distal part of the sciatic nerve at earlier time points after injury, would shed light on whether FAP-derived BDNF can also contribute to axon regeneration in addition to remyelination. Unfortunately, we could not perform such additional experiments within the limited time frame, since preparing enough numbers of control and conditional knockout mice that match the age groups used in this study (3-4 months old), followed by waiting for additional 2-4 weeks after nerve crush injury for sample collection, and subsequent immunostaining for quantification could take almost 6 months in total. We hope that the Reviewer understands this limitation.

- (b) We appreciate the Reviewer's constructive comment. Although the number of animals used for neuromuscular junction (NMJ) analyses was not sufficient, we had briefly examined the structure of NMJs at 4 weeks post nerve crush injury in control (Ctrl) and conditional

knockout (cKO) mice as a preliminary experiment. As a result, no significant differences were observed between Ctrl and cKO mice in terms of NMJ morphology and innervation (Author response image 3).

Author response image 3.

Structures of neuromuscular junctions from Ctrl vs cKO mice at 4 weeks post nerve crush injury. Whole-mount immunostaining was done using the exterior digitorum longus muscles that were affected by sciatic nerve crush injury. Samples were stained with α -bungarotoxin (green), neurofilament (red), and synaptophysin (blue). Scale bar: 50 μ m.



Going back to part (a) of this Reviewer's comment, considering the data presented in Author response image 3, where innervation of axons into acetylcholine receptor clusters was not significantly different between Ctrl versus cKO mice, FAP-derived BDNF may not be critical for the axonal growth upon nerve injury. Although we acknowledge that additional experiments are required to draw a meaningful conclusion on this point, we could not perform such additional experiments due to insufficient time and resources.

We hope that the Reviewer understands our limitation.

Recommendations for the authors:

[1] In citing the ability of BDNF to promote Schwann cell myelination the authors should include Chan et al., 2001 (PMID 11717413) in addition to the Zhang et al, 2000 and Xiao et al, 2009 references.

- We apologize for missing out the reference mentioned by the Reviewer. We have added the suggested reference in our revised manuscript (lines 395, 425, and 517).

Reviewer #2

Public review:

[1] Although, I find the data the authors generated enough for their claims. I do see them as relatively poor, and (a) a complementary analysis of protein expression would strengthen the paper through immunostaining of the different genes mentioned for FAPs and Schwann cells. The model is entirely supported by measuring mRNA levels and negative regulation of gene expression in specific cells. Additionally, (b) what happens to the structure of the neuromuscular junction after regeneration when GDNF or BDNF expression is reduced? (c) The determination of decreasing levels of FAPs BDNF mRNA during aging is interesting; is the gain of BDNF expression in FAPs reverting the phenotype?

- (a) We appreciate and agree with the Reviewer's comment that validation of BDNF protein expression in FAPs and GDNF protein expression in Schwann cells upon nerve injury would strengthen this paper. Regarding GDNF protein expression in Schwann cells upon nerve injury, it has already been demonstrated by previous studies (Höke et al., 2002; Xu et al., 2013). For BDNF protein expression in FAPs upon nerve injury, we performed western blot analysis for validation, as mentioned in the response to Reviewer #1 Public review [2]. The results showed that while the mature form of BDNF protein could not be readily detected in FAPs isolated from uninjured muscles, it could be detected in FAPs isolated from sciatic nerve crush injury-affected muscles at 7 days post injury. We have added the new result as Figure 4F in the New Figure 4 with the experimental scheme as New Figure 4—figure supplement 1, and revised the Results section (lines 364-374) and the Materials and Methods section (lines 687-705) in our manuscript to include the new results in detail.

- (b) Though the data is preliminary, we examined the structures of neuromuscular junctions (NMJs) from control and *Prrx1Cre; Bdnf fl/fl* mice at 4 weeks post injury in the exterior digitorum longus muscles, as mentioned in the response to Reviewer #1 Public review [4](b). As a result, we could not identify significant differences between control versus *Prrx1Cre; Bdnf fl/fl* mice, where BDNF expression is reduced specifically in *Prrx1*-expressing cells, including FAPs (Attached Figure 3). Since other cellular sources of BDNF, such as Schwann cells, exist, regeneration of the NMJs may not have been as significantly affected as remyelination in our *Prrx1Cre; Bdnf fl/fl* mice. However, further experiments with a sufficient number of mice and more observation time points are required to statistically validate this hypothesis in detail. Unfortunately, preparing samples for such additional analyses would take more than four months, as we need to produce sufficient numbers of control and *Prrx1Cre; Bdnf fl/fl* mice that match the age groups used in this study. We hope that the Reviewer understands our limitation.

Regarding analyzing NMJ structures after regeneration affected by reduced GDNF levels, using genetic models such as *Plp1CreER; Gdnf fl/fl* mice would be appropriate, as we have used the *Prrx1Cre; Bdnf fl/fl* mice in this study to reduce BDNF levels produced by FAPs. Unfortunately, we do not have the *Gdnf fl/fl* mice, and obtaining these mice to produce *Plp1CreER; Gdnf fl/fl* mice and performing the additional experiment would take too much time for this current revision. In a further study, we will try to perform the additional experiment by obtaining the required mouse line. We hope that the Reviewer understands our limitation.

- (c) We appreciate the Reviewer for highlighting this point. In this paper, we have shown that BDNF expression upon nerve injury is decreased in aged FAPs compared to young adult FAPs, and suggested that this may be one of the causes of the delayed nerve regeneration phenotype in aged mice. Previously, it has been reported that while intramuscular injection of BDNF accelerates nerve regeneration, intramuscular injection of anti-BDNF antibodies delays the regeneration process (Zheng et al., 2016). This implies that intramuscular levels of active BDNF can significantly influence the speed of nerve regeneration. Therefore, the gain of BDNF expression in aged FAPs may contribute to reversing the delayed nerve regeneration phenotype in aged mice, since it would result in additional supply of active, intramuscular BDNF, which has previously been shown to accelerate nerve regeneration. Though experimental validation is required to support such claim, we could not obtain sufficient numbers of aged mice within the limited time frame. We hope that the Reviewer understands our limitation.

Recommendations for the authors:

[1] The authors should include the experimental design and several drawings in the leading figures indicating, for example, how remyelination after injury was quantified

and how the response of regenerated sciatic nerve to a depolarizing stimulus was studied.

- We apologize for any confusion caused by insufficient information provided in the leading figures. Unfortunately, due to limited space, we could not add experimental designs or drawings in the leading figures. Instead, to do our best to comply with the

Reviewer's comment, we have revised the figure legends in the leading figures so that the experimental designs or diagrams can be referred to in the figure supplements.

We hope that the Reviewer understands this limitation.

Reviewer #3

Public review:

[1] In Fig. 1 and 2 authors provide data on scRNA seq and this is important information reporting the finding of RET and GFRA1 transcripts in the subpopulation of FAP cells. However, authors provide no data on the expression of RET and GFRA1 proteins in FAP cells.

- Reply for this comment by the Reviewer is in the Recommendations for the authors section below ([2]), as the same comment is repeated.

[2] Another problem is the lack of information showing that GDNF secreted by Schwann cells can activate RET and its down-stream signaling in FAP cells. There is no direct experimental proof that GDNF activating GFRA1-RET signaling triggers BDNF upregulation in FAP cells. The data that GDNF signaling is inducing the synthesis and secretion of BDNF is also not conclusive.

- Reply for this comment by the Reviewer is in the Recommendations for the authors section below ([3]), as the same comment is repeated.

Recommendations for the authors:

[1] Although this is a novel study and contains very well-performed parts, the GDNF section is preliminary and requires additional experimentation. In the introduction authors describe well FAPs but even do not mention how GDNF is signaling. Moreover, the reader may get an impression that Ras-MAPK pathway is the only or at least the main GDNF signaling pathway. In fact, for neurons Akt and Src signaling pathways play also crucial role.

- We apologize for the missing content in the Introduction section of our manuscript and for any confusion caused by our misleading description of the GDNF signaling pathway. We have revised our manuscript to include the GDNF signaling pathway in the Introduction section, along with a description of other downstream signaling pathways of GDNF that are known to play crucial roles, as mentioned by the Reviewer (lines 115-130). Additionally, we changed the expression in the Results section to avoid making any misleading impressions (lines 318-319).

[2] In Fig. 1 and 2 authors provide data on scRNA seq and this is important information reporting the finding of RET and GFRA1 transcripts in the subpopulation of FAP cells. However, authors provide no data on the expression of RET and GFRA1 proteins in FAP cells.

- We appreciate the Reviewer for the constructive comment. Though we fully agree with the Reviewer that validating the expression of RET and GFRA1 proteins in FAPs is needed, we

were unable to obtain the antibodies required for such experiments within the limited time frame for this revision. We hope that the Reviewer understands our limitation. Although we could not directly show the expression of those GDNF receptor genes at the protein level in FAPs, based on the result where intramuscular GDNF injection could sufficiently induce *Bdnf* expression in FAPs compared to PBS control in the absence of nerve damage, it is likely that GDNF receptors are indeed expressed at the protein level in FAPs, since if otherwise, FAPs would not have been able to respond to the injected GDNF protein. Nevertheless, in a future study, we will try to validate the protein-level expression of GDNF receptors in FAPs to comply with the Reviewer's suggestion and to further support this study.

[3] Another problem is the lack of information showing that GDNF secreted by Schwann cells can activate RET and its down-stream signaling in FAP cells. Authors can monitor activation of MAPK pathway by detecting phospho-Erk and PI3 kinase-Akt pathway measuring phospho-S6 using immunohistochemistry. We can recommend to use the following antibodies: pErk1/2 (1:300, Cell Signaling, Cat# 4370L RRID:AB_2297462), pS6 (1:300, Cell Signaling, Cat# 4858L RRID:AB_1031194). These experiments are crucial because RET and GFRA1 proteins maybe not expressed at the sufficient level on the cell surface.

- We sincerely appreciate the Reviewer's constructive comment. In this study, we suggested that the GDNF-BDNF axis within FAPs would signal through the MAPK pathway based on the bioinformatic analysis of our single cell RNA-seq data and matching the results with the previously known pathways. We fully agree that monitoring the activation of the MAPK pathway and the PI3K-Akt pathway by immunohistochemistry would experimentally demonstrate whether GDNF can activate those pathways within FAPs through GFRA1/RET activation. Unfortunately, we could not obtain the antibodies suggested by the Reviewer for this revision due to insufficient research funds and limited time frame. We hope that the Reviewer understands our limitation. In future studies, we will try to validate the detailed molecular pathway that mediates the GDNF-BDNF axis in FAPs by incorporating the methodology suggested by the Reviewer, along with implementation of genetic models such as *Plp1CreER*; *Gdnf^{fl/fl}*, *Prrx1Cre*; *Ret^{fl/fl}* or *Prrx1Cre*; *Gfra1^{fl/fl}* to validate whether Schwann cell-derived

GDNF can actually signal through its canonical receptor RET/GFRA1 expressed in FAPs to induce expression of BDNF upon nerve injury.

[4] (a) There is no direct experimental proof that GDNF activating GFRA1-RET signaling triggers BDNF upregulation in FAP cells. Authors can use GDNF blocking antibodies, siRNA or use RET or GFRA1 cKO mice to delete them from FAP cells. (b) The data that GDNF signaling is inducing the synthesis and secretion of BDNF is also not conclusive. Authors should show that GDNF injection is increasing BDNF protein levels in FAPs. To get sufficient material for ELISA detection of BDNF is perhaps problematic. However, authors can use BDNF antibodies from Icosagen company and use IHC.

- (a) We appreciate the Reviewer for the critical comment. As mentioned in the reply for Reviewer #1 Public review [3], we used GDNF blocking antibodies to reduce GDNF signaling within the tibialis anterior and gastrocnemius muscles by intramuscular injection after sciatic nerve crush injury, and included the result as a new figure supplement in our revised manuscript (New Figure 4—figure supplement 2) with its details in both the Results section (lines 381-390) and the Materials and Methods section (lines 611-616). Though the results were not statistically significant, intramuscular injection of anti-GDNF antibodies showed a tendency toward reduced *Bdnf* expression in FAPs, compared to IgG controls. As mentioned in the reply for Reviewer #1 Public review [3], and as suggested by the Reviewer, using cKO mice such as *Plp1CreER*; *Gdnf^{fl/fl}*, *Prrx1Cre*; *Ret^{fl/fl}*, or *Prrx1Cre*; *Gfra1^{fl/fl}* mice would further

validate the GDNF-BDNF axis suggested in this study, likely with statistical significance. Unfortunately, obtaining these genetic models within the limited time frame of this current revision is not feasible. We will try to adopt such models in our future study to validate the role of Schwann cell-derived GDNF in inducing BDNF expression in FAPs via activation of RET/GFR α 1.

- (b) We appreciate the Reviewer for the constructive comment. Though we fully agree that the experiment suggested by the Reviewer would validate the synthesis and secretion of BDNF protein by GDNF signaling in FAPs, we were not able to perform it due to lack of research funds to obtain enough amount of the GDNF protein. We hope that the Reviewer understands our limitation. Still, combining the results from New Figure 4H in this study with the New Figure 4F, where GDNF injection induced *Bdnf* mRNA expression in FAPs, and BDNF protein expression in FAPs in response to nerve injury was demonstrated via western blot, we anticipate that GDNF injection would increase BDNF protein levels in FAPs, though direct validation of this statement would require conducting the additional experiments mentioned by the Reviewer.

References

Chan JR, Cosgaya JM, Wu YJ, and Shooter EM (2001). Neurotrophins are key mediators of the myelination program in the peripheral nervous system. *Proceedings of the National Academy of Sciences* 98:14661-14668.

English AW, Liu K, Nicolini JM, Mulligan AM, and Ye K (2013). Small-molecule trkB agonists promote axon regeneration in cut peripheral nerves. *Proc Natl Acad Sci U S A* 110:16217-22.10.1073/pnas.1303646110

Giordani L, He GJ, Negroni E, Sakai H, Law JY, Siu MM, Wan R, Corneau A, Tajbakhsh S, and Cheung TH (2019). High-dimensional single-cell cartography reveals novel skeletal muscle-resident cell populations. *Molecular Cell* 74:609-621. e6.

Höke A, Gordon T, Zochodne D, and Sulaiman O (2002). A decline in glial cell-linederived neurotrophic factor expression is associated with impaired regeneration after long-term Schwann cell denervation. *Experimental neurology* 173:77-85.

Kim J-H, Kang J-S, Yoo K, Jeong J, Park I, Park JH, Rhee J, Jeon S, Jo Y-W, and Hann S-H (2022). Bap1/SMN axis in Dpp4⁺ skeletal muscle mesenchymal cells regulates the neuromuscular system. *JCI Insight* 7:

Leinroth AP, Miranda AJ, Rouse D, Kobayashi Y, Tata PR, Rueckert HE, Liao Y, Long JT, Chakkalakal JV, and Hilton MJ (2022). Identification of distinct non-myogenic skeletal-muscle-resident mesenchymal cell populations. *Cell Reports* 39:

Liu L, Cheung TH, Charville GW, and Rando TA (2015). Isolation of skeletal muscle stem cells by fluorescence-activated cell sorting. *Nature protocols* 10:1612-1624.

Oudega M, and Hagg T (1998). Neurotrophins promote regeneration of sensory axons in the adult rat spinal cord. *Brain Research* 818:431-438.10.1016/S0006-8993(98)01314-6

Xiao J, Wong AW, Willingham MM, Kaasinen SK, Hendry IA, Howitt J, Putz U, Barrett GL, Kilpatrick TJ, and Murray SS (2009). BDNF exerts contrasting effects on peripheral myelination of NGF-dependent and BDNF-dependent DRG neurons. *J Neurosci* 29:4016-22.10.1523/JNEUROSCI.3811-08.2009

Xu P, Rosen KM, Hedstrom K, Rey O, Guha S, Hart C, and Corfas G (2013). Nerve injury induces glial cell linederived neurotrophic factor (gdnf) expression in schwann cells through purinergic signaling and the pkcpkd pathway. *Glia* 61:1029-1040.

Zhang JY, Luo XG, Xian CJ, Liu ZH, and Zhou XF (2000). Endogenous BDNF is required for myelination and regeneration of injured sciatic nerve in rodents. *European Journal of Neuroscience* 12:4171-4180.10.1111/j.1460-9568.2000.01312.x

Zheng J, Sun J, Lu X, Zhao P, Li K, and Li L (2016). BDNF promotes the axonal regrowth after sciatic nerve crush through intrinsic neuronal capability upregulation and distal portion protection. *Neuroscience letters* 621:1-8.

<https://doi.org/10.7554/eLife.97662.2.sa0>